STUDY ON SOME METHODOLOGIES ON DIRECT TORQUE CONTROL OF PERMANENT MAGNET SYNCHRONOUS MOTOR FOR MINIMIZING TORQUE RIPPLE

A thesis is submitted to fulfil the requirement of the degree

Master in Electrical Engineering

Submitted by

SK Nasim Ali

Examination Roll no. – **M4ELE22015**

Registration no. – **154005** of **2020-2021**

Year – **2nd**, Semester – **4th**

Under the guidance of

Prof. Susanta Ray

and

Prof. Arabinda Das

Department of Electrical Engineering

Jadavpur University

Kolkata – 700032

August 2022

Faculty of Engineering and Technology
Jadavpur University, Kolkata - 700032

Certificate

This is to certify that the thesis entitled **"Study on Some Methodologies on Direct Torque Control of Permanent Magnet Synchronous Motor for Minimizing Torque Ripple"**, submitted by **Mr SK Nasim Ali** (Examination Roll No. M4ELE22015), under our supervision and guidance during the session of 2020-22 in the department of Electrical Engineering, Jadavpur University. We are satisfied with his work, which is being presented for the partial fulfilment of the degree of **Master in Electrical Engineering** from Jadavpur University, Kolkata-700032.

……..

Prof. Susanta Ray
Associate Professor
Department of Electrical Engineering
Jadavpur University
Kolkata, 700032

……

Prof. Arabinda Das
Professor
Department of Electrical Engineering
Jadavpur University
Kolkata, 700032

……

Prof. Chandan Mazumdar
Dean of Faculty Council of
Engineering and Technology
Jadavpur University
Kolkata, 700032

……

Prof. Saswati Mazumdar
Head of the Department of
Electrical Engineering
Jadavpur University
Kolkata, 700032

Faculty of Engineering and Technology
Jadavpur University, Kolkata - 700032

Certificate of Approval

The forgoing thesis entitled **"Study on Some Methodologies on Direct Torque Control of Permanent Magnet Synchronous Motor for Minimizing Torque Ripple"** is hereby approved as a creditable study of an Engineering subject carried out and presented in a manner that fulfils its acceptance as a prerequisite to the degree for which it is submitted. It is understood that by this approval, the undersigned does not necessarily endorse or approve any statement made, opinion expressed, or conclusion drawn therein but approves the thesis only for the purpose for which it is submitted.

The final examination for evaluation of the thesis

Signature of the examiners

……

……

……

Declaration of Originality

I hereby declare that this thesis contains a literature survey and original research work done by me. All the information in this document has been obtained and presented according to academic rules and ethical conduct. I also declare that, as required by these rules and conduct, I have fully cited and referenced all material and results that are not original to this work.

Name: SK NASIM ALI

Examination Roll No: M4ELE22015

Thesis Title: Study on Some Methodologies on Direct Torque Control of Permanent Magnet Synchronous Motor for Minimizing Torque Ripple.

Signature with Date:

ACKNOWLEDGEMENTS

I express my sincere gratitude to my supervisor**, Prof. Susanta Ray** for his encouragement, suggestion and advice, without which it would not have been possible to complete my thesis successfully. I would like to thank **Prof. Arabinda Das** for being a constant source of encouragement, inspiration and for his valuable suggestions coupled with his technical expertise throughout my research work. It was a great honour for me to pursue my research under his supervision.

I would also like to thank my co-worker Aritra Pal, all the staff of the Drives and Simulation laboratory, and the research scholars of our department for providing constant encouragement throughout my thesis work.

Last but not least I extend my words of gratitude to my parents for personally motivating me to carry out the work smoothly.

ABSTRACT

This thesis studies the mathematical model of Permanent Magnet Synchronous Motor (PMSM), a general idea of the Direct Torque Control (DTC) method, a DTC based on duty ratio modulation, and a new approach for modification of duty ratio modulation-based DTC using Maximum Torque Per Ampere (MTPA) scheme. Space Vector Modulation (SVM) is used to choose the inverter's voltage vectors for various time periods. Look-Up Table (LUT) is used to choose the voltage vectors for various values of torque and flux with various phases. And then simulations of the PMSM drive are accomplished with the two methods mentioned above in the MATLAB® SIMULINK environment. Then the ripples produced in speed and torque response of DTC with duty ratio modulation and DTC with modified duty ratio modulation are compared. The fact that DTC has large torque and current ripple makes it clear that it has a particular disadvantage. The Modified Duty Ratio Modulated Technique is an effective solution to this issue. This thesis work supports the claim that the modified duty ratio modulated method is preferable for significantly reducing the ripple percentage. It can reduce the torque ripple as well when there are load variations.

List of Acronyms

Short Form	Full-Form
AC	Alternating Current
PMSM	Permanent Magnet Synchronous Motor.
DC	Direct Current
PM	Permanent Magnet
SCR	Silicon-Controlled Rectifier
EMF	Electro-Motive Force
D-Q	Direct-Quadrature
FOC	Field Oriented Control
DTC	Direct Torque Control
LUT	Look-Up Table
PWM	Pulse Width Modulation
IM	Induction Motor
SVM	Space Vector Modulation
MTPA	Maximum Torque Per Ampere
SPM	Surface-mounted Permanent Magnet
SIPM	Surface Inset Permanent Magnet
IPM	Interior Permanent Magnet
MMF	Magneto Motive Force
VSI	Voltage Source Inverter
GTO	Gate Turn Off thyristor
BJT	Bipolar Junction Transistor
MOSFET	Metal Oxide Semiconductor Field Effect Transistor
IGBT	Insulated Gate Bipolar Junction Transistor
SV-PWM	Space Vector- Pulse Width Modulation
PI	Proportional Integral
SPMSM	Surface Mounted Permanent Magnet Synchronous Machine
PMACM	Permanent Magnet Alternating Current Motor

List of Symbols

Symbols	Meaning
L_d	Inductance along D-axis
L_q	Inductance along Q-axis.
N_s	Synchronous speed
f	Frequency
P	Pole pair
θ_r	Angle between rotor reference frame and fixed stator axis
v_q, v_d	Stator voltages along Q and D axis
v_a, v_b, v_c	Stator voltage along A, B and C axis
Ψ_r	Rotor flux
Ψ_a, Ψ_b, Ψ_c	Stator flux along A, B and C axis
Ψ_d, Ψ_q	Stator flux along D and Q axis
L_{kk}	Self-inductance of the k-th phase
L_{ij}	Mutual inductance of i-th phase due to j-th phase
i_a, i_b, i_c	Stator current along A, B and C axis
i_d, i_q	Stator current along D and Q axis
R_s	Stator resistance
ω_s	Stator synchronous speed
P_{in}	Input power
P_{out}	Output power
T_e	Electro-magnetic torque
T_L	Load torque
J	Moment of inertia
B	Viscous co-efficient
ω_r	Rotor speed
S_A, S_B, S_C	Switching pulse of the leg, A, B and C
ψ^s	Stator flux
δ	Load angle
i_α, i_β	Stator current along α and β
v_α, v_β	Stator voltage along α and β
α	The angle between two components of the stator flux vector
ψ_{ref}	Reference flux
ψ_{err}	Flux error
H_ψ	Flux hysteresis limit
H_T	Torque hysteresis limit

t_k	On-time
t_0	Off-time
T_H	Torque hysteresis bandwidth
ΔT_m	Torque error
T_s	Sample time
C	Constant
d	Duty ratio

List of Figures

List of Tables

Chapter 1

Introduction and Literature Review

A device known as a permanent magnet synchronous motor is one that incorporates permanent magnets within the steel rotor in order to generate a magnetic field that is continuous. This motor is ideal for a wide range of motion control applications.

A revolving magnetic field is created by the stator windings connected to an AC source. After that, the rotor poles align themselves in synchronous motion with the rotating magnetic field. The most frequent magnets utilised in these motors are neodymium magnets.

1.1 History of Permanent Magnets Machines

In the 1950s, the availability of modern permanent magnets with a high energy density prompted the creation of dc machines with permanent magnet field excitation. The employment of permanent magnets (PMs) to replace electromagnetic poles with windings that required an electric energy supply source eventually led to the development of DC machines. Similarly, in synchronous machines, the PM poles replace the traditional electromagnetic field poles in the rotor, eliminating the need for slip rings and brush assemblies [1].

The mechanical commutator was replaced with an electronic commutator in the form of an inverter with the introduction of switching power transistors and silicon-controlled rectifier devices in the late 1950s. PMSMs were developed as a result of these two advancements. If the mechanical commutator is replaced by an electronic equivalent, the armature of the dc machine does not need to be on the rotor. As a result, the machine's armature may be mounted upon the stator, allowing for greater cooling and higher voltages due to the stator's large clearance room for insulation. These machines are basic examples of what is known as "an inside out dc machine," in which the field and armature are reversed, moving from the stator to the rotor and then from the rotor to the stator, respectively [1] [2].

The rotor of PMSM provides a constant magnetic field, but it requires a variable magnetic field to start, hence these motors need a variable frequency power supply. Permanent magnet synchronous motors require a driver to function; they cannot function without one [2].

Since the back EMF of the PMSM is sinusoidal, sinusoidal stator currents are required to keep the torque constant. PMSM is virtually identical to a wound rotor synchronous machine, with the two primary distinctions being that the PMSMs often lack damper windings and rely on a permanent magnet for excitation instead of a field winding. D-Q mathematical model of PMSM was constructed from the Synchronous Motor model using this theory, by omitting equations of damper winding dynamics and field current dynamics. This model was first proposed by R. Krishnan and P. Pillay; in 1988 [3].

1.2 Motivation of Work

Permanent magnet synchronous motor drives are replacing the traditional Induction motor and dc motor drives and becoming popular in most industries due to their several advantages.

But the main drawback of PMSM is speed control. Because Controlling the AC supply that is on the stator is the only way to regulate this motor since there is only one source, which is the AC supply that is on the stator. A sophisticated control system, complete with power electronics and microcontrollers, is essential for this.

In the latter half of the 1950s, technological advancements led to the creation of new devices that were based on the switching power transistor and silicon-controlled rectifiers, after these many control techniques were proposed but the most common and popular two techniques are FOC and DTC. After comparing DTC and FOC we can see DTC, unlike FOC, does not need the use of a current regulator, coordinate transformation, or a PWM signal generator. Besides its simplicity, it provides an extremely high dynamic torque response. Furthermore, in comparison to FOC, the Direct torque controller is less sensitive to machine parameters. Only stator resistance is required to implement this type of control [4].

Despite its many advantages, one major drawback of DTC is its high current and torque ripple. In this thesis, a DTC technique is proposed using duty ratio modulation to reduce torque ripple. The main task of this process is to determine the duty ratio. The motive of this work is to propose a technique which can reduce the torque ripple more than the previously used technique. Also, a simulation in MATLAB Simulink has been carried out to prove the effectiveness of this model.

1.3 Literature Review

After the advancement of the AC drives Induction motors were being used extensively in many industries due to their robustness. Also, the absence of brushes, commutators, and slip rings makes the motor cheaper and maintenance-free. But the major drawback of this machine is lower efficiency and power-to-weight ratio.

To overcome these drawbacks PMSM drives were introduced in the 1950s. Nowadays PMSMs are replacing IM drives in industries like machine positioning, robotics, electric and hybrid vehicles, aeronautic systems, etc. due to its several structural and operational features like 1). the capacity to work at various speeds, 2). higher efficiency than IM due to less heat generation, 3). higher power density due to smaller size, 4). lower cost of maintenance due to emission of brushes, 5). higher torque-to-current ratio. 6). higher power factor [1].

But one major challenge for PMSM drives was controlling their speed there were many techniques to control the speed of AC drives like Variable frequency SCR inverter with auxiliary current circuit and feedback current transformer [5]. Also, there is a technique where Pulse Width Modulated Inverters are used to obtain variable frequency-variable voltage [6]. But all these techniques were less efficient and de-coupling between flux and electromagnetic torque does not exist in those techniques.

In order to get a decoupled control between flux and electromagnetic torque DTC was first introduced by I. Takahashi and T. Noguchi, in 1986 [7]. The findings of this paper show that this control method has outstanding torque response and efficiency characteristics, proving its validity with a simpler structure. After that, a High-Performance Direct Torque Control method was proposed by I. Takahashi and Y. Ohmori [8]. In this method, the torque response of the system was improved by using two sets of three-phase inverters. Instantaneous voltage vectors applied by an inverter give some degree of flexibility in determining the switching modes of a power converter. High-speed torque control and main flux management are made possible via the use of this switching flexibility. T. G. Habetler and D. M. Divan followed their work and proposed a direct torque control scheme using discrete pulse-modulated inverters [9]. The use of only one current sensor in the DC connection makes this control mechanism unique. H. Y. Zhong, H. P. Messinger and M. H. Rashad made some further improvements in this field and proposed a microcomputer-based direct primary flux and torque control system [10]. Using a non-zero space voltage vector and its time breadth, they demonstrated that the main flux

amplitude could be modified, as could the electromagnetic torque amplitude. Over time many other DTC techniques were proposed like DTC using space vector modulation, and DTC using PWM inverter [11]-[12]. In 1997 DTC was first investigated on PMSM by L. Zhong, M. F. Rahman *et al*. They used mathematics to demonstrate that the increase in electromagnetic torque in a permanent magnet motor is proportional to the increase in the angle between the stator and rotor flux linkages. As a result, they demonstrated that the rapid torque response could be achieved by modifying the rotational speed of the stator flux linkage in the shortest amount of time possible. It is also proved that zero voltage vectors should not be used and that the stator flux linkage should always be moving in proportion to the rotor flux linkage. Both of these findings are supported by the evidence presented here [13]. The conventional direct torque control does not require any motor parameter except the stator resistance. Using this flux and Electromagnetic torque are estimated and compared with the reference value. Also, two hysteresis controllers are used here according to the output of these two controllers and the position of the flux vector an appropriate voltage vector is selected from a switching table according to the voltage vector the switching state of the inverter is selected. In 1999 [14] L. Zhong, M. F. Rahman *et al.* implemented their investigation of DTC on a prototype PMSM which has a standard induction motor stator. They also derived the switching table specific for an interior PMSM.

Out of a few drawbacks, one of the major drawbacks in the DTC of PMSM is torque ripple. In order to solve this problem, several techniques were proposed. In [15] a sensor-less technique is proposed. Also, in several studies, Space Vector Modulation (SVM) [16] is used to generate continuous voltage vectors that can correctly and moderately modify torque and flux. However, the rotary coordinate transformation is required in SVM-based DTC schemes, which is more computationally complex than standard DTC.

Another process to reduce torque ripple in DTC is using a multi-level inverter [17]. An asymmetric cascaded multilayer inverter generates the voltage vector without the requirement for modulation or filtering. Here the torque ripple is minimized due to the higher output quality of the inverter but the cost of hardware is very much high for this process.[18].

Another method is duty cycle control, which is used in traditional DTC in order to reduce the torque ripple. In traditional DTC a voltage vector is applied for the whole period of time which results in the torque and flux value increasing over the reference value and which ultimately

causes torque ripple. Each sample period in this approach uses both an active vector and a zero vector. Duty cycle control was first proposed by Pengcheng Zhu, Yong Kang and Jian Chen in 2003 [19]. First, it was implemented in the Induction motor. The main task of this method is to determine the duty ratio. Later D. -H. Lee, Y. -J. An and E. -C. Nho proposed a method for determining the duty ratio for PMSM drive [20]. In this method, the duty ratio is determined by the torque error and torque bandwidth. But the major drawback of this method is the torque ripple is dependent on the hysteresis band. With the increase and decrease of the hysteresis band, the torque ripple is also increased or decreased. In order to make it independent of the torque hysteresis band, a new method was proposed by I. R. Akhil and C. K. Vijayakumari [21]. Here the duty ratio is established only on the basis of torque error. So, here the ripple content can be reduced independent of the bandwidth of the torque hysteresis controller.

In this paper, a relation between torque and flux has been established using the MTPA equation used in [22] and the torque is calculated by converting the estimated flux using that equation. After that comparing with reference torque, the torque error has been generated and the duty ratio has been calculated using that torque error. This method gives a reduction in torque ripple.

All the simulations are done in MATLAB Simulink and compared with other methods under the same circumstances. The results are also provided here which show a significant reduction in torque ripple.

1.4 Organization of Thesis

The thesis is structured as follows:

- **Chapter 1** outlines the preliminary concept of thesis work. It contains a brief history of permanent magnet machines, my motivation for this work and the review of different literature available on the above-mentioned topic and their limitations are also discussed here.
- **Chapter 2** contains detailed information about PMSM. Stator and rotor construction, the working principle and the complete mathematical model of PMSM are discussed here.

- **Chapter 3** consists of detailed information regarding the voltage source inverter. Also, the power devices used in the voltage source inverter, VSI topology and the switching states of the inverter are discussed here.
- In **chapter 4** Direct Torque control is discussed in detail. After giving a brief introduction to DTC the basic principle of DTC and control topology is discussed here. Then a schematic diagram for conventional DTC is shown and discussed here.
- **Chapter 5** discusses the duty ratio modulation technique. After that reason for using this method and how it is applied are discussed. Then the method for calculating the duty ratio is also described here. At last, a schematic diagram using this technique is shown and discussed here.
- In **chapter 6,** the maximum torque per ampere scheme is discussed here basis principle for MTPA is discussed. Then a relationship between torque and flux is established using MTPA.
- **Chapter 7** contains the proposed method which is used in this work. Also, a schematic diagram of the proposed method is shown and discussed here.
- **Chapter 8** is the most important chapter where the responses obtained from MATLAB for all the important parameters for all cases have been shown. Then the responses are compared with each other and the ripple percentages and observations from the results are discussed.
- **Chapter 9** is the conclusion of this thesis. Here, my contributions to project work and the future scopes that may come from my work are discussed.

Chapter 2

Permanent Magnet Synchronous Motor

2.1 Introduction

The Permanent Magnet Synchronous Motor (PMSM) is a type of Synchronous motor in which permanent magnets are used to energise the rotor field. It is brushless with very high reliability and efficiency. Permanent magnets are utilised to produce a spinning magnetic field rather than winding for the rotor. This kind of motor does not need a DC source to power the rotor. Because there is no DC supply, these motors are simple and inexpensive. As a general principle, it is an AC-synchronous motor with a sinusoidal back EMF waveform that is powered by permanent magnets. In order to create torque at zero speed, the PMSM relies on permanent magnets. A digitally controlled inverter is required for this motor to perform at its peak efficiency [23] [24].

2.2 Construction of PMSM

The stator and rotor are the two primary components of PMSM. The armature winding of the motor is done by the stator, which is the part that doesn't move. The field winding is done by the rotor. The armature winding is the main winding because it induces EMF in the motor. The field winding is carried by the rotor the main field flux is induced in the rotor through permanent magnets. Material with excellent permeability and coercivity is used in the construction of these Permanent Magnets These materials are Samarium-Cobalt and Neodymium-Iron-Boron.[24][25].

2.2.1 Rotor construction

As discussed earlier the rotor of PMSM is made of a permanent magnet. Generally, rare earth material with high coercive force is used as permanent magnets. According to the shape design of the rotor, the rotors are specified into two types [26]:

1. Salient pole rotor

2. Non-salient pole rotor.

The non-salient pole rotors are cylindrical in shape. For this type of rotor, there is a uniform air gap, between the stator and rotor. Due to this uniform air gap, the direct and quadrature axis inductances of this type of rotor are equal ($L_d = L_q$) [26].

The Salient pole-type rotors do not have a uniform air gap between stator and rotor. So, for this kind of rotor, the direct and quadrature axis inductances are not equal $(L_d \neq L_q)$ [26].

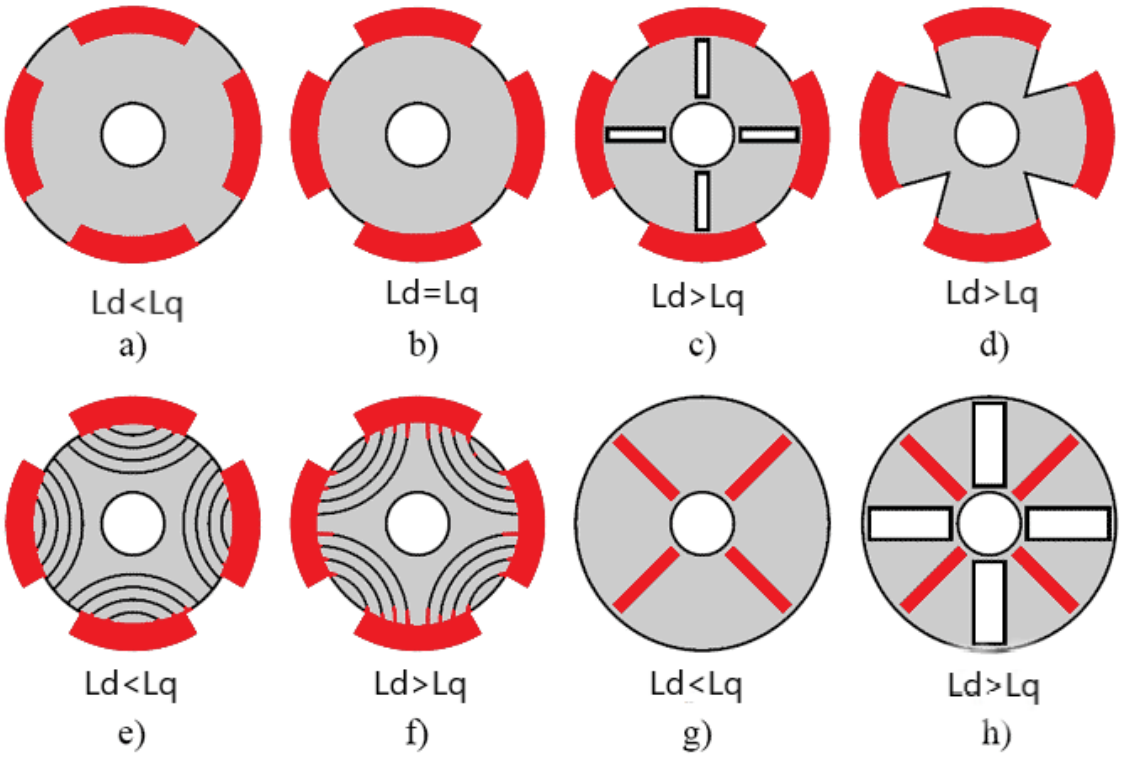

Fig2.1 Rotor cross sections with varying L_d/L_q ratios. Magnets marked red. Fig. e & f shows rotors that are layered axially. Fig. c & h shows how the rotors are blocked.

According to the arrangement of the permanent magnet in the rotor, there are several types of rotor. Here, we talk about some of the most common arrangements and how they affect the airgap flux density, winding inductances, and reluctance torque.

1. Surface-Mounted PMSM: In this type of setup, the magnets are attached to the surface of the rotor laminations on the outer edge. This kind of arrangement doesn't get interrupted by anything else, like rotor lamination. It has the maximum air gap flux density because it confronts the air gap directly. However, this kind of design has several drawbacks. This kind of configuration has a poor level of structural integrity and mechanical toughness. In practice, PMs are buried into the rotor laminations using Kavaler tape. So that it can provide some mechanical strength. Also, the magnets are bound to the rotor. So, it reinforces the mechanical

strength of the rotor. These arrangements are not preferred for high-speed applications. The difference in reluctance between the direct and quadrature axes in this machine is very small because it is built like a non-salient pole. The variation between the quadrature and direct axes inductances is less than 10% [1] [2].

2. Surface-Inset PMSM: In this kind of set-up, the magnets are put in the grooves around the outside of the rotor laminations. Because of this, it gives the rotor a smooth, round surface. This setup is much more mechanically stable than the last one. The magnets are fully and mechanically embedded in the rotor which gives it mechanical strength from flying out. In this machine, the difference between the inductances of the quadrature and direct axes can be as high as 2–2.5 [1] [2].

3. Interior PMSM: In this type of setup, the magnets are placed in the middle of the rotor laminations in either a radial or circumferential direction. This design is strong in terms of mechanics, so it can be used for high-speed applications. This set-up is harder to make than magnet rotors that are surface mounted or set inside a housing. Note that the ratio between the inductances of the quadrature and direct axes is between 3 and 1. But there have been claims that other interior PM rotor configurations have a much higher ratio [2].

In this kind of set-up, sometimes some steel is taken out of the rotor to make big air gaps between the magnets in the rotor. This is done to stop flux from moving from one PM to the next on the upper rotor surface. The flux will move from one magnet to the next one in the rotor, bypassing the structure of the stator. This means that there will be fewer mutual flux linkages. The weight of the rotor also becomes less which gives the lowest rotor inertia. So, it provides higher acceleration rates.

Another type of inset rotor is the circumferential interior PM rotor. It requires a large volume of PMs. So, this setup can only be used with low-cost, low-energy magnets like ferrites, since high-energy magnets are expensive. In this setup, the air gap flux density can be made higher because the cross-sectional area of the magnets is much bigger than the surface area of the rotor that carries the flux from a magnet to the stator. Because of the higher air gap flux

density, this setup is very desirable from the viewpoint of better efficiency and relatively small stator excitation for the same power output [1] [2].

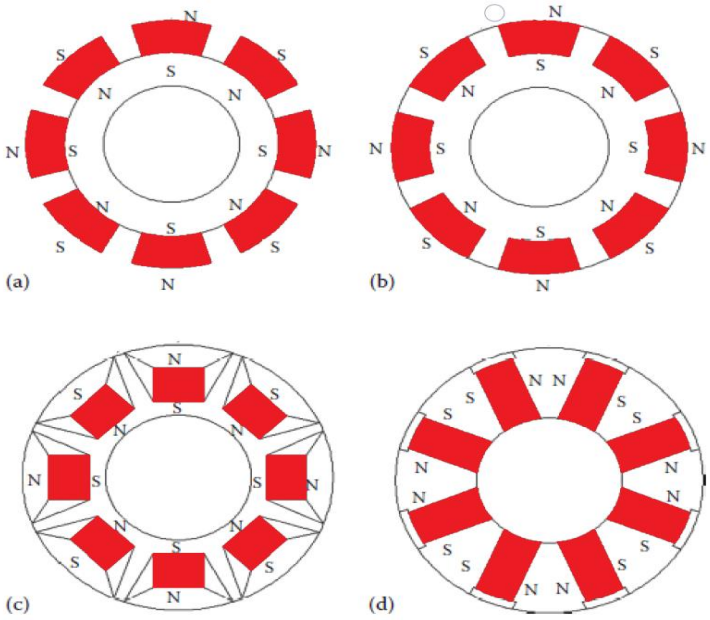

Fig 2.2. Types of PMSM. (a) Surface mounted PMSM. (b) Surface inset PMSM. (c) Interior PMSM. (d) Interior PMSM with circumferential orientation

2.2.2 Stator construction

The stator is constructed with two parts at the outmost surface there is an outer frame. This has a core with windings inside of it. Windings with two or three phases are the most prevalent.

The two kinds of permanent magnet synchronous motors are distinguished by the stator design:

1. PMSM with a distributed winding

2. PMSM with a concentrated winding [26].

1. Distributed winding: In this type of winding the number of slots per pole and phase Q = 2, 3, ..., k.

2. Concentrated winding: The number of slots per pole and phase is Q = 1 in this type of winding. The slots on this stator are uniformly spaced all the way around its circumference. These windings are made up of two coils that can be linked either in parallel or in series. The main problem with these windings is that you can't change the shape of the EMF curve [25][26].

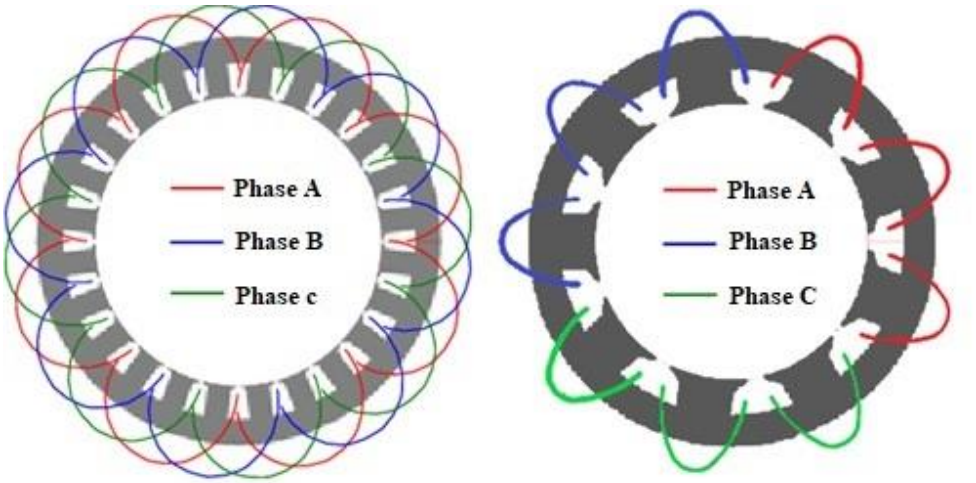

Fig 2.3 (a) Distributed windings. (b)Concentrated windings.

2.3 Working Principle of PMSM

Compared to other conventional motors the working of the permanent magnet synchronous motor is very simple, fast, and effective. The Working Principle of PMSM is based on the interaction of the rotating magnetic field generated via stator due 3 phase supply and the constant magnetic field of the rotor generated via permanent magnet.

The rotating magnetic field in the air gap via stator is generated in the same way as in a 3-phase induction motor. The generated rotating magnetic field revolves in synchronous speed and it can be calculated by, $N_s = 120 * f/P$ this equation here f denotes the frequency of supply and P denotes the number of poles.

By joining the windings of the stator with one another phasor groups are created and by joining these phasor groups to gather different connections like a star, Delta, double and single phases are formed. The windings are wound shortly with each other to reduce harmonic voltages.

The permanent magnets used as the rotor creates a constant magnetic flux. When the constant magnetic field of the rotor locks with the rotating magnetic field in the air gap generated by the stator the rotor starts to rotate at synchronous speed. The rotor rotates at synchronous speed

regardless of the applied load torque. When the applied load torque crosses the maximum limit, the rotor becomes standstill [24][25][26].

2.4 Mathematical Modelling of PMSM

Here, a complete mathematical model of the motor is derived for proper simulation and analysis of the system. For ease of calculation, the motor axis has been developed using the d-q rotor reference frame theory [3]. The rotor reference frame makes an angle θ_r with the fixed stator axis at any time instance t. The stator MMF makes an angle α with the rotor d-axis, and at any time t, the stator MMF spins at the very same speed as the rotor axis [1].

There are some assumptions made in the process:

1) Saturation isn't taken into account, but parameter changes can do that;

2) The Induced EMF is sinusoidal in nature;

3) Eddy current and hysteresis losses are insignificant.

4) No field current dynamics.

2.4.1 Three-phase to two-phase transformations (ABC to DQ)

It can be done by changing the voltages and currents of the three phases ABC to $\alpha\beta$ axis variables by using the Clarke transformation, $f_{\alpha\beta} = K_1.f_{abc}$. After that to transform it from $\alpha\beta$ to d-q Clarke transformation is used, $f_{qd} = K_2.f_{\alpha\beta} = K_2.K_1.f_{abc} = K.f_{abc}$. D-Q Modelling of the system is used to study the motor in both the steady state and the transient state [28].

$$K_1 = \frac{2}{3}.\begin{bmatrix} 1 & -\frac{1}{2} & -\frac{1}{2} \\ 0 & \frac{\sqrt{3}}{2} & -\frac{\sqrt{3}}{2} \\ \frac{1}{2} & \frac{1}{2} & \frac{1}{2} \end{bmatrix} \quad (2.1)$$

$$\text{and, } K_2 = \begin{bmatrix} \cos\theta & -\sin\theta & 0 \\ \sin\theta & \cos\theta & 0 \end{bmatrix} \quad (2.2)$$

Hence, K can be calculated as,

$$K = \frac{2}{3}.\begin{bmatrix} \cos(\theta) & \cos(\theta - \frac{2\pi}{3}) & \cos(\theta + \frac{2\pi}{3}) \\ \sin(\theta) & \sin(\theta - \frac{2\pi}{3}) & \sin(\theta + \frac{2\pi}{3}) \end{bmatrix} \quad (2.3)$$

Consequently,

$$K^{-1} = \begin{bmatrix} \cos(\theta) & \sin(\theta) \\ \cos(\theta - \frac{2\pi}{3}) & \sin(\theta - \frac{2\pi}{3}) \\ \cos(\theta + \frac{2\pi}{3}) & \sin(\theta + \frac{2\pi}{3}) \end{bmatrix} \quad (2.4)$$

Three phase voltages (v_a, v_b, v_c) of the inverter are converted to $D-Q$ axis voltages (v_d, v_q) by using the Park transformation shown below [1][3]:

$$\begin{bmatrix} v_q \\ v_d \\ v_0 \end{bmatrix} = \frac{2}{3}\begin{bmatrix} \cos(\theta) & \cos(\theta - \frac{2\pi}{3}) & \cos(\theta + \frac{2\pi}{3}) \\ \sin(\theta) & \sin(\theta - \frac{2\pi}{3}) & \sin(\theta + \frac{2\pi}{3}) \end{bmatrix}\begin{bmatrix} v_a \\ v_b \\ v_c \end{bmatrix}$$

The inverse Park transformation, as stated below, is used to derive abc variables from d, q variables [1].

$$\begin{bmatrix} v_a \\ v_b \\ v_c \end{bmatrix} = \begin{bmatrix} \cos(\theta) & \sin(\theta) \\ \cos(\theta - \frac{2\pi}{3}) & \sin(\theta - \frac{2\pi}{3}) \\ \cos(\theta + \frac{2\pi}{3}) & \sin(\theta + \frac{2\pi}{3}) \end{bmatrix}\begin{bmatrix} v_q \\ v_d \\ v_0 \end{bmatrix}$$

2.4.2 Motor modelling

The equivalent circuit model based on d and q-coordinates is used to model PMSMs. A conceptual cross-sectional image of a 3-phase, 2-pole interior PMSM is shown in Fig. 2.4, along with two reference frames. We assume that the permanent magnet rotor generates magnetic flux in the direction of the d-axis Ψ_r.

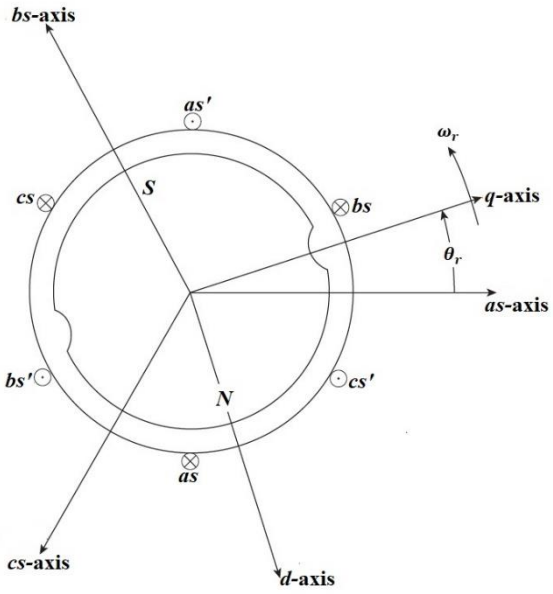

Fig 2.4 Motor axis

Along the a-phase, b-phase, and c-phase axes of the stator, the components of this rotor flux are, $\Psi_r \cos(\theta)$, $\Psi_r \cos(\theta - \frac{2\pi}{3})$ and $\Psi_r \cos(\theta + \frac{2\pi}{3})$ respectively. Thus, phase flux linkages can be expressed as [1]:

$$\Psi_a = L_{aa}.i_a + L_{ab}.i_b + L_{ac}.i_c + \Psi_r.\cos(\theta) \quad (2.5)$$

$$\Psi_b = L_{ba}.i_a + L_{bb}.i_b + L_{bc}.i_c + \Psi_r.\cos(\theta - \frac{2\pi}{3}) \quad (2.6)$$

$$\Psi_c = L_{ca}.i_a + L_{cb}.i_b + L_{cc}.i_c + \Psi_r.\cos(\theta + \frac{2\pi}{3}) \quad (2.7)$$

Here,L_{kk} is the self-inductance of the k-th phase and L_{ij} is the mutual inductance of the i-th phase due to the j-th phase.

Due to the balanced mode of PMSM with symmetrical alignments of the inductances, we can consider,

$$L_{kk} = L \text{ for } k = a, b \text{ or } c$$

$$L_{ij} = L_m \text{ for all } i \text{ and } j .$$

So, in a balanced condition, the sum of the stator currents equal to zero, i.e. $i_a + i_b + i_c = 0$,

Due to these, the simplified phase flux linkage equations provide the following results:

$$\Psi_a = (L - L_m).i_a + \Psi_r.\cos(\theta) \tag{2. 8}$$

$$\Psi_b = (L - L_m).i_b + \Psi_r.\cos\left(\theta - \frac{2\pi}{3}\right) \tag{2. 9}$$

$$\Psi_c = (L - L_m).i_c + \Psi_r.\cos\left(\theta + \frac{2\pi}{3}\right) \tag{2. 10}$$

The stator phase voltages in balanced mode may now be expressed as,

$$v_a = R_s.i_a + \frac{d\Psi_a}{dt} \tag{2. 11}$$

$$v_b = R_s.i_b + \frac{d\Psi_b}{dt} \tag{2. 12}$$

$$v_c = R_s.i_c + \frac{d\Psi_c}{dt} \tag{2. 13}$$

If we consider, $[f_{abc}] = [f_a \ f_b \ f_c]^T$, then the above set of equations can be written as

$$[v_{abc}] = R_s.I_{3\times3}.[i_{abc}] + \frac{d}{dt}[\Psi_{abc}] \tag{2. 14}$$

and essentially the expression of $[\Psi_{abc}]$ is as,

$$[\Psi_{abc}] = (L - L_m).I_{3\times3}.[i_{abc}] + \Psi_r.[A_{cos}] \tag{2. 15}$$

where we have, $[A_{cos}] = \begin{bmatrix} \cos(\theta) \\ \cos\left(\theta - \frac{2\pi}{3}\right) \\ \cos\left(\theta + \frac{2\pi}{3}\right) \end{bmatrix}$

Now the transformation of $[\Psi_{abc}]$ to $[\Psi_{dq}]$reference frame is done,

$$[\Psi_{dq}] = (L - L_m).I_{2\times2}.[i_{dq}] + \Psi_r.\begin{bmatrix}0\\1\end{bmatrix} \tag{2. 16}$$

And, to frame $[v_{dq}]$ can be written as

$$\left[v_{dq}\right] = R_s.I_{2\times2}.\left[i_{dq}\right] + K.\frac{d}{dt}K^{-1}[\,\Psi_{dq}\,] \qquad (2.\ 17)$$

Following fundamental calculus on matrix- expressions we get,

$$\frac{d}{dt}K^{-1}\left[\Psi_{dq}\right] = \left[\frac{d}{dt}K^{-1}\right].\left[\Psi_{dq}\right] + \ K^{-1}.\frac{d}{dt}\left[\Psi_{dq}\right]$$

Hence, $K.\frac{d}{dt}K^{-1}[\,\Psi_{dq}\,]$ is expressed as,

$$K.\frac{d}{dt}K^{-1}\left[\Psi_{dq}\right] = K.\left[\frac{d}{dt}K^{-1}\right].\left[\Psi_{dq}\right] + \frac{d}{dt}\left[\Psi_{dq}\right]$$

Following simple calculations we have,

$$K.\left[\frac{d}{dt}K^{-1}\right] = \begin{bmatrix}0 & -1\\ 1 & 0\end{bmatrix}.\frac{d\theta}{dt} = \begin{bmatrix}0 & -1\\ 1 & 0\end{bmatrix}.\omega_s$$

Following fundamental calculus on matrix- expressions we get,

$$\frac{d}{dt}K^{-1}\left[\Psi_{dq}\right] = \left[\frac{d}{dt}K^{-1}\right].\left[\Psi_{dq}\right] + \ K^{-1}.\frac{d}{dt}\left[\Psi_{dq}\right]$$

Hence, $K.\frac{d}{dt}K^{-1}[\,\Psi_{dq}\,]$ is expressed as,

$$K.\frac{d}{dt}K^{-1}\left[\Psi_{dq}\right] = K.\left[\frac{d}{dt}K^{-1}\right].\left[\Psi_{dq}\right] + \frac{d}{dt}\left[\Psi_{dq}\right]$$

Following simple calculations we have,

$$K.\left[\frac{d}{dt}K^{-1}\right] = \begin{bmatrix}0 & -1\\ 1 & 0\end{bmatrix}.\frac{d\theta}{dt} = \begin{bmatrix}0 & -1\\ 1 & 0\end{bmatrix}.\omega_s$$

Finally, the expression of $\left[v_{dq}\right]$ becomes,

$$\left[v_{dq}\right] = .I_{2\times2}.\left[i_{dq}\right] + (L - L_m).I_{2\times2}.\frac{d}{dt}\left[i_{dq}\right] \ + \begin{bmatrix}0 & -1\\ 1 & 0\end{bmatrix}.\omega_s.\ \left[\Psi_{dq}\right] \qquad (2.\ 18)$$

$$[\Psi_{dq}] = (L - L_m).I_{2\times2}.[i_{dq}] + \Psi_r.\begin{bmatrix}0\\1\end{bmatrix} \quad (2.\ 19)$$

this implies,

$$\begin{bmatrix}0 & -1\\1 & 0\end{bmatrix}.\omega_s.\ [\Psi_{dq}] = \begin{bmatrix}-(L - L_m).\omega_s.i_q\\(L - L_m).\omega_s.i_d + \omega_s.\Psi_r\end{bmatrix} \quad (2.\ 20)$$

And finally substituting this in the expression of $[v_{dq}]$we get,

$$v_d = R_s.i_d - (L - L_m).\omega_s.i_q + (L - M).\frac{di_d}{dt} \quad (2.\ 21)$$

$$v_q = R_s.i_q + (L - L_m).\omega_s.i_d + (L - M).\frac{di_q}{dt} + \omega_s.\Psi_r \quad (2.\ 22)$$

We are considering the balanced mode, and so we may consider, $(L - L_m) = L_d = L_q$ and this reveals the expression of v_d and v_q as,

$$v_d = R_s.i_d - L_q.i_q.\omega_s + L_d.\frac{di_d}{dt} \quad (2.\ 23)$$

$$v_q = R_s.i_q + L_d.i_d.\omega_s + L_q.\frac{di_q}{dt} + \omega_s.\Psi_r \quad (2.\ 24)$$

To define the flux linkage of the transformed axes, we follow,

$$\begin{bmatrix}0 & -1\\1 & 0\end{bmatrix}.\omega_s.\ [\Psi_{dq}] = \begin{bmatrix}-(L - L_m).\omega_s.i_q\\(L - L_m).\omega_s.i_d + \omega_s.\Psi_r\end{bmatrix}$$

Which implies,

$$[\Psi_{qd}] = \begin{bmatrix}\Psi_q\\\Psi_d\end{bmatrix} = \begin{bmatrix}L_q.i_q\\L_d.i_d + \Psi_r\end{bmatrix} \quad (2.\ 25)$$

Therefore, following equation (3) the dynamic equivalent circuit of PMSM in the d-q frame can be depicted as,

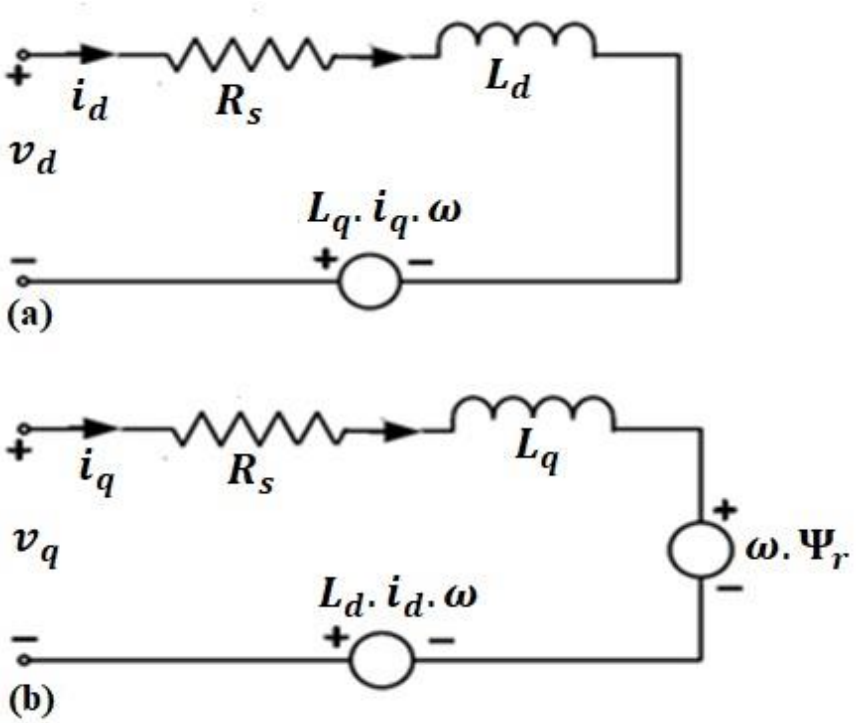

Fig:2.5 (a) D-axis circuit and (b) Q-axis circuit

2.4.3 Electromagnetic torque equation

We ignore the magnetic field saturation situation, as well as losses owing to eddy currents and hysteresis, in order to suggest power invariant transformation. And we obtain:

$$P_{in} = P_{out} = \frac{3}{2}\left(v_q . i_q + v_d . i_d\right) \quad (2.\ 26)$$

Substituting the values of v_q and v_d we get,

$$P_{out} = \frac{3}{2}\left(\Psi_d . i_q - \Psi_q . i_d\right). \omega_s \quad (2.\ 27)$$

Therefore, the total electrical torque is expressed as,

$$T_e = (Pole\ Pair). \frac{P_{0ut}}{\omega_s} = P\ . \frac{3}{2} . \left(\Psi_d . i_q - \Psi_q . i_d\right) \quad (2.\ 28)$$

Substituting the values of Ψ_d and Ψ_q we get,

$$T_e = P.\frac{3}{2}.\left(\{L_d - L_q\}.i_d.i_q + \Psi_r.i_q\right) \quad (2.29)$$

2.4.4 Mechanical system model

The system's load torque, accelerating torque, and damping torque balance the electromagnetic torque, which may be expressed as [22] [27]:

$$T_e = T_L + B.\omega_r + J.\frac{d}{dt}\omega_r \quad (2.30)$$

Here T_L is the load torque, B is the damping coefficient and J is the moment of inertia.

$$\omega_s = (Pole\ Pair).\omega_r$$

2.4.5 Final modelling equation

For the purpose of dynamic simulation, the equations can be re-arranged to give first-order nonlinear differential equations in terms of variables as [22],[27]:

$$\frac{d}{dt}i_d = (v_d - R_s.i_d + \omega_s.L_q.i_q)/L_d \quad (2.31)$$

$$\frac{d}{dt}i_q = (v_q - R_s.i_q - \omega_s.L_d.i_d - \omega_s\Psi_r)/L_q \quad (2.32)$$

$$\frac{d}{dt}\omega_r = (T_e - T_L - B.\omega_r)/J \quad (2.33)$$

$$\omega_r = \int \frac{(T_e - T_L - B.\omega_r)}{J}\, dt \quad (2.34)$$

$$\frac{d}{dt}\theta_s = \omega_s \quad (2.35)$$

Combining the set of equations, we can develop a complete states space dynamic model of PMSM in the d-q reference frame.

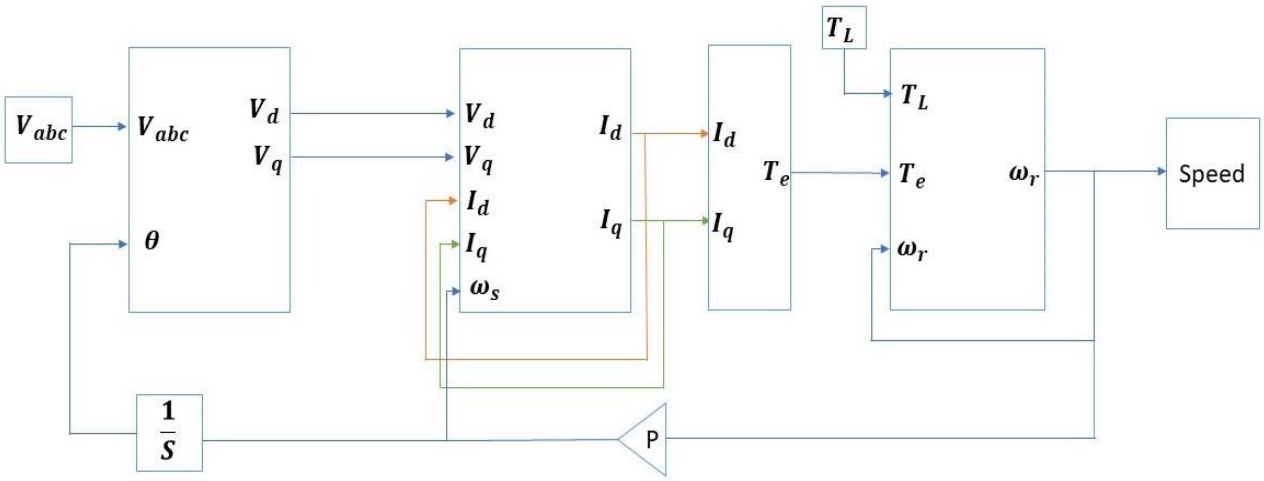

Fig 2.6 Simulink-based block diagram of PMSM drive system

Chapter 3

Voltage Source Inverter

3.1 Introduction

The standard power electronic inverter modules are the subsystem that allowed the widespread usage of permanent magnet (PM) drives practicable. Inversion is the process of converting dc to alternating current power, and it is the inverter that generates the variable frequency from the dc source that is utilized to drive a permanent magnet synchronous motor at a variable speed [1].

For the process of DTC, a three-phase voltage source inverter with a 180-degree conduction mode is used here.

3.2 Power Devices Used in VSI

Voltage, current, power, and frequency control have all become more affordable since the invention of semiconductor power switches. Some power electronic devices that are used as active switches in VSI are:

- Diode
- Thyristor or silicon-controlled rectifier (SCR)
- Gate Turn off Thyristor (GTO)
- Bipolar junction transistor (BJT)
- Power MOSFET
- Insulated Gate Bipolar Junction Transistor (IGBT)

These power electronic devices are generally used as a switch of VSI.

3.3 VSI Topology

The usage of three-phase bridge inverters for general-purpose ac supply and ac motor drives is very common. The voltage source inverter (VSI) is generally utilized in the DTC. VSI may be a two-level or multi-level inverter, but this work will concern a two-level type as it is the most common type. In figure 3.1 the basic topology of the inverter is shown. Figure 3.2

Explains how the square wave, or six-step, mode of operation generates the output voltage waves. To create the three-phase voltage waves, the circuit consists of three half-bridges that are phase-shifted by an angle of $2\pi/3$ [30].

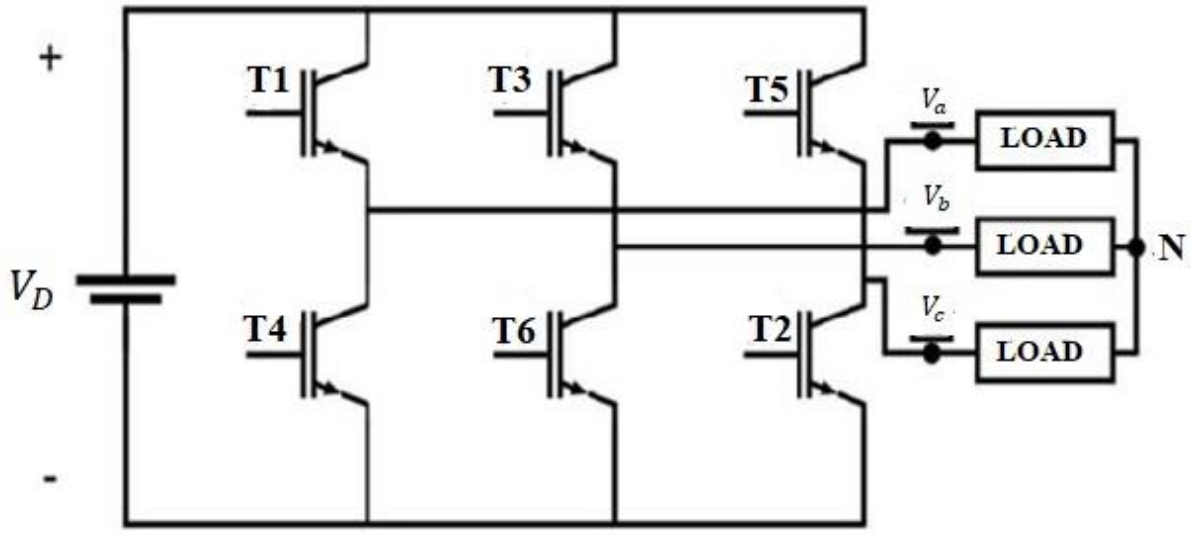

Figure 3.1 Topology of voltage source inverter

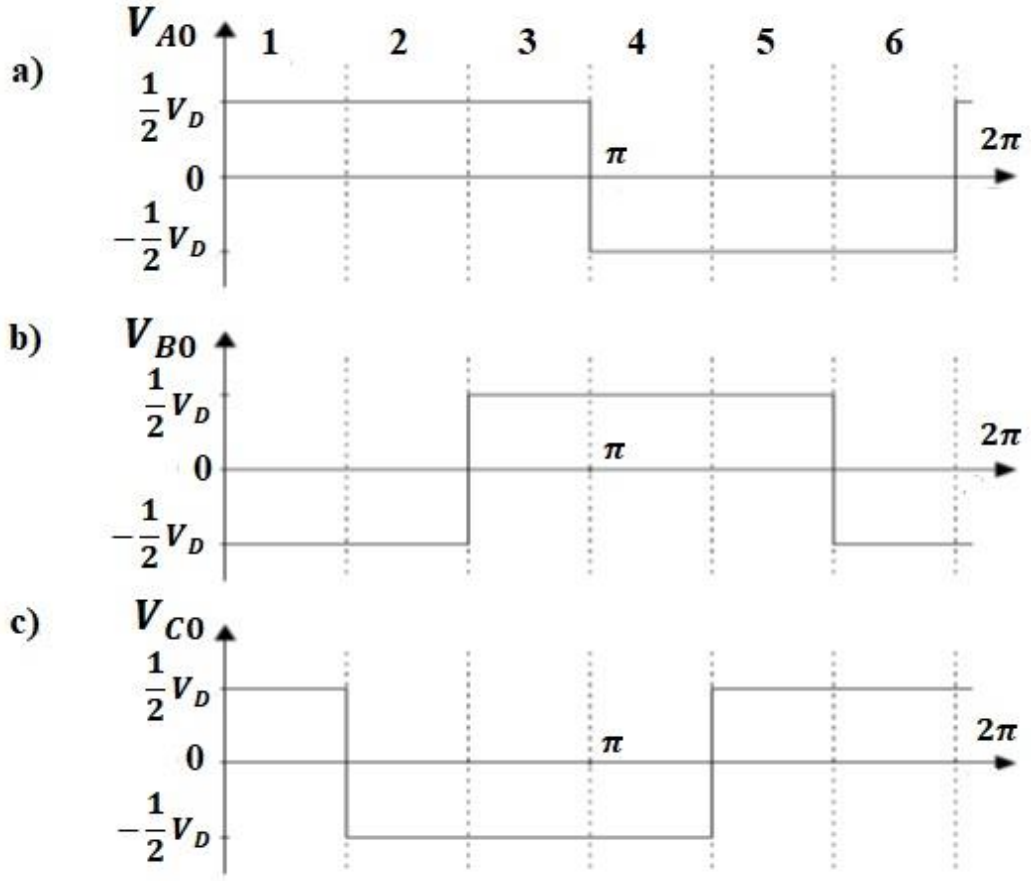

Figure 3.2 Phase voltages for 180-degree conduction mode

The six switches are divided into two groups. The top three switches (S1, S3, and S5) make up the positive group, and the bottom three switches make up the negative group (i.e., S4, S6, S2). Six of the eight possible switching states (1–6) are active and produce non-zero ac output voltages. The other two states have no voltage (0 and 7) [30].

State	S_A	S_B	S_C	**Vector**
0	0	0	0	V_0
1	1	0	0	V_1
2	1	1	0	V_2
3	0	1	0	V_3
4	0	1	1	V_4
5	0	0	1	V_5
6	1	0	1	V_6
7	1	1	1	V_7

Table 3.1 Switching state of 3-phase voltage source inverter

3.4 Switching States of VSI

The three-phase stator voltages of the motor V_A, V_B and V_c are decided by the states of the 3 switches S_A, S_B and S_c. If S_A is 1 that means V_A is connected to the +ve terminal of DC supply and if S_A is 0 that means V_A is connected to the -ve terminal of DC supply. The same cases are for V_B and V_c. For example, if (S_A, S_B, S_c) = (1,0,0) then V_A is connected to the +ve terminal of the battery and both V_B and V_c are connected to the –ve terminal. The resultant voltage vector (V_1,) can be calculated as [29]:

$$V_1 = \frac{2}{3}V_D + \frac{1}{3}V_D.\cos 60 + \frac{1}{3}V_D.cos\,60 = V_D \tag{3.1}$$

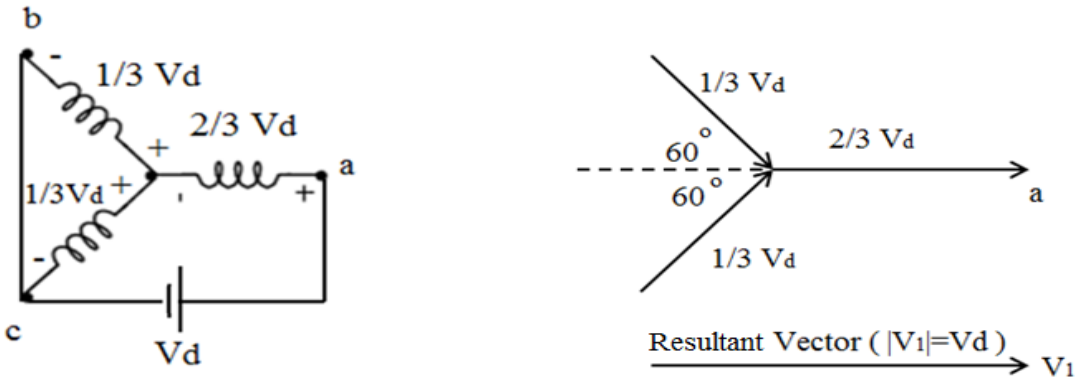

Figure 3.3 The resultant voltage vector of the switching status (1, 0, 0)

For the switching status (1, 1, 0), both V_A and V_B are connected to the +ve terminal of V_D and V_c is connected to the –ve terminal. The resultant voltage vector has a magnitude of V_D and 60° apart from the reference (Phase a). The resultant voltage vector (V_2) can be calculated as [29]:

$$V_2 = \frac{2}{3}V_D\angle 60° + \frac{1}{3}V_D + \frac{1}{3}V_D\angle 120° = V_D\angle 60° \tag{3.2}$$

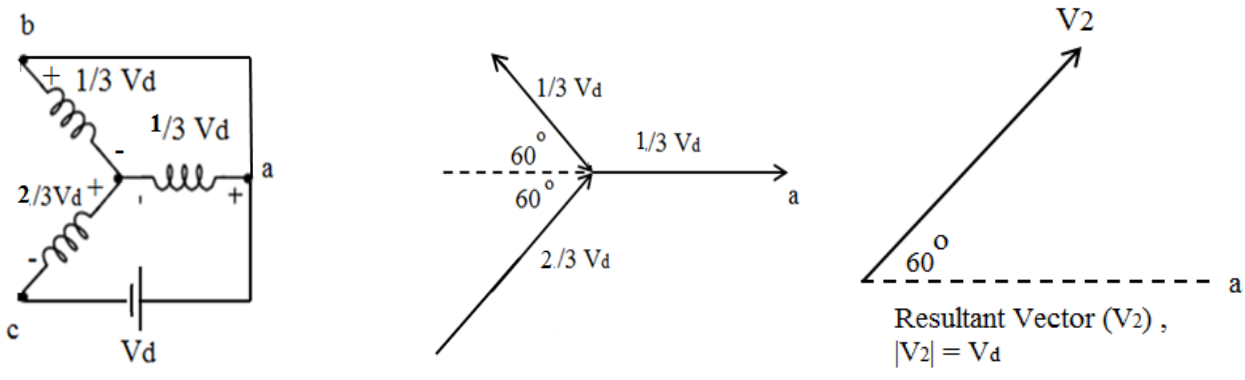

Figure 3.4 The resultant voltage vector of the switching status (1, 1, 0)

Therefore, there are eight voltage vectors, six are non-zero voltage vectors (active voltage vectors): V_1 (100), V_2 (110), V_3 (010), V_4(011), V_5 (001), and V_6 (101) and two zero voltage vectors V_0 (000) and V_7 (111).

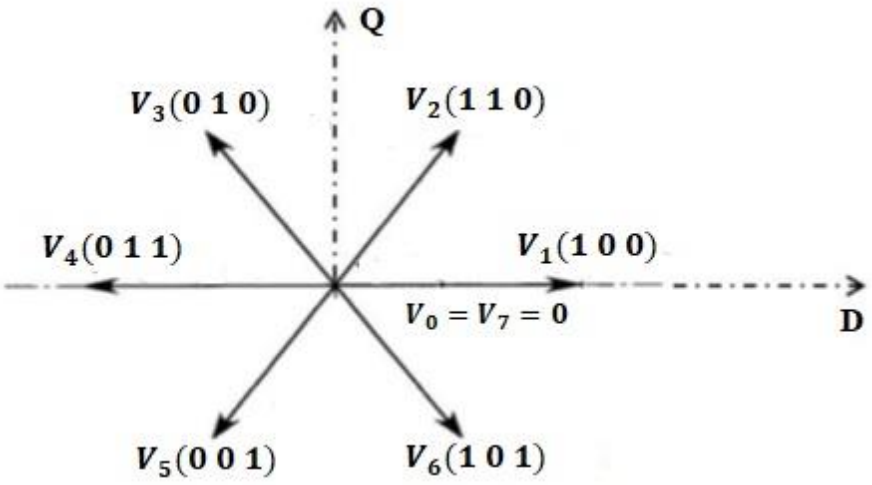

Figure 3.5 Inverter eight voltage vectors in D-Q plane

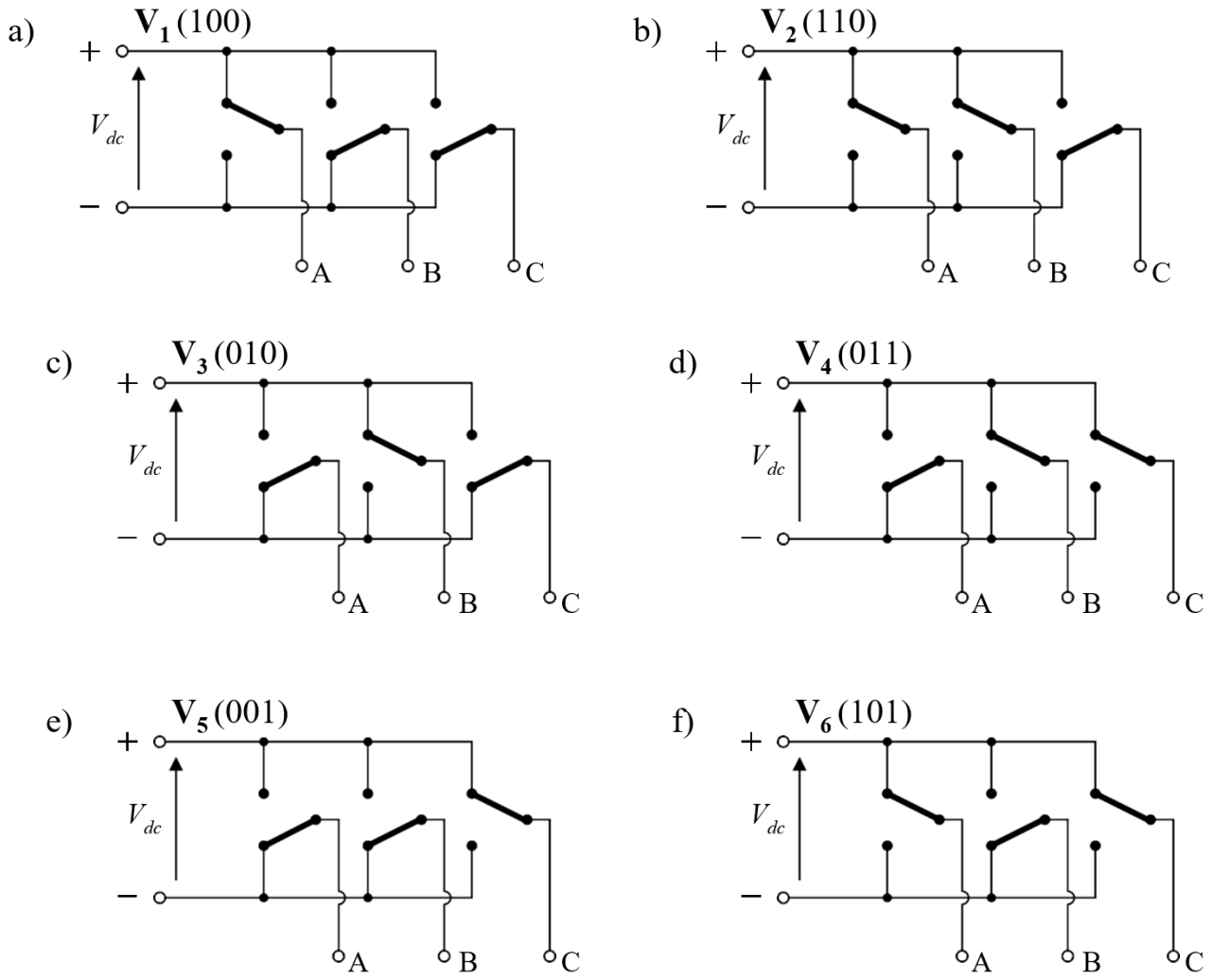

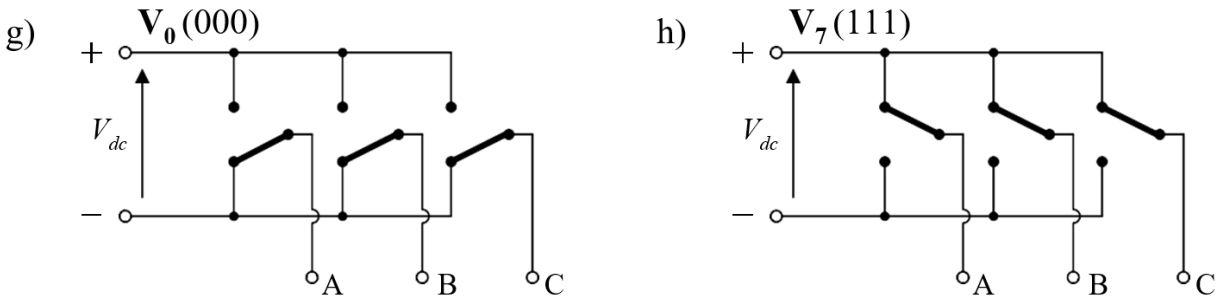

Figure 3.6 Switching states for VSI

A method known as space vector pulse width modulation can be used to combine the non-zero voltage vectors and the zero voltage vectors to produce additional voltage vectors that are different from these eight vectors (SV-PWM). The average of the needed voltage vector in SV-PWM should match the average of the voltage the inverter produces.

The needed voltage vector is created by applying two non-zero voltage vectors for times T1 and T2, respectively, and a zero-voltage vector for time T0, where the total of these times T1, T2, and T0 equals the sampling time Ts. We may derive the times T1 and T2 by equating the "Volt. Sec." in both the D- and Q-planes. T0 is obtained by subtracting T1 and T2 from Ts.

Chapter 4

Conventional Direct Torque control

4.1 Introduction

The conventional DTC system is a closed loop control scheme with the following key elements: a motor, a three-phase voltage source inverter and a speed controller to provide the torque command included in this power supply circuit. The underlying principle of DTC is to directly choose the stator voltage vectors based on the disparities between the reference and real torque and flux values. Nonlinear transformations on hysteresis controllers are used to directly regulate and resolve torque and flow without requiring coordinate transformations [31].

The DTC controller is comprised of stator flux estimate blocks, 2 different hysteresis controllers, and a sector selection block. The DTC controller sends gating pulses to the inverter.

Because all control actions are performed in a stationary frame of reference, the DTC system does not need coordinate transformation. As a result, this system is not as susceptible to parameter fluctuations as other control techniques. There is also no feedback current control loop, thus control operations are not delayed as they are with current controllers. Also, there is no pulse width modulator, PI controller, rotor speed or position sensor. So, it is a sensor-less control system because it doesn't need a mechanical sensor on the shaft to run the motor. To close the loop, online torque and flux estimators are utilised. Here, hysteresis comparators are used to directly regulate the torque and stator flux [32].

The interaction of stator and rotor fields produces the governing equation for torque in this design. Torque and stator flux linkage is calculated using motor terminal data such as stator voltages and current. The hysteresis control of stator flux and torque selects an appropriate voltage vector for VSI switching from among six nonzero voltage vectors and two zero voltage vectors.

This control approach entails a comparative control of the torque and stator flux. It is more commonly used in regulating electrical machines since it is a simple and durable approach. Because the stator current and voltage are regulated indirectly, no current feedback loops are necessary. The block diagram of conventional DTC is given in Fig. 4.1.

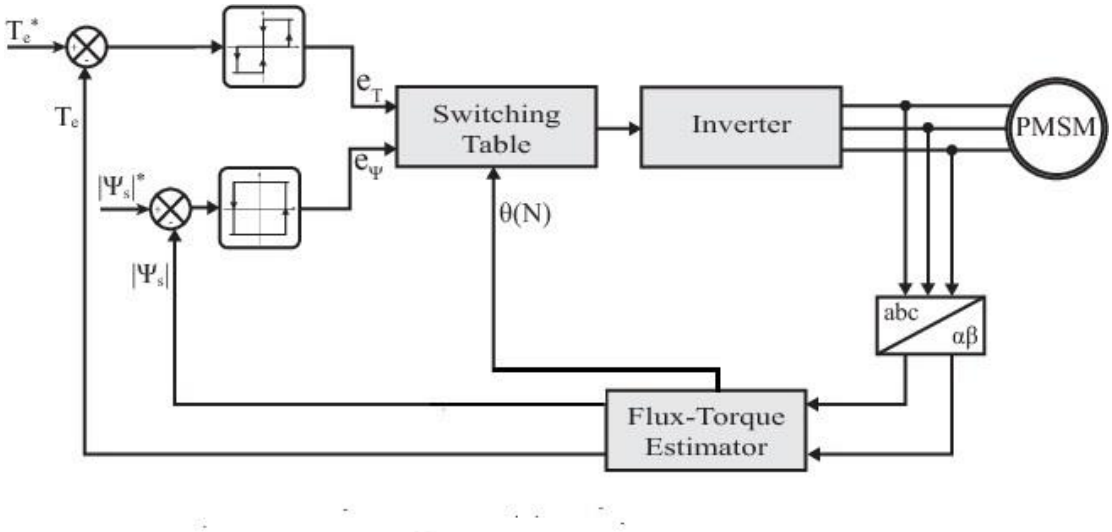

Figure 4.1 Conventional direct torque control

4.2 Principal of DTC

In PMSM stator flux can be calculated using the equation below:

$$\psi^s = \int (v_s - R_s . i_s) dt \tag{4.1}$$

Here v_s and i_s denotes stator voltage and current respectively and R denotes the resistance of the stator windings.

The stator flux may be characterised as the time integration of the stator voltage, ignoring the stator resistance voltage drop. As the motor is powered by a 3- Phase voltage supply the motor flux will build up in the direction of the voltage vector. The stator voltage vector may be any of the six non-zero vectors in Fig 4.2 or zero at any time if the inverter is operated in a certain switching mode.

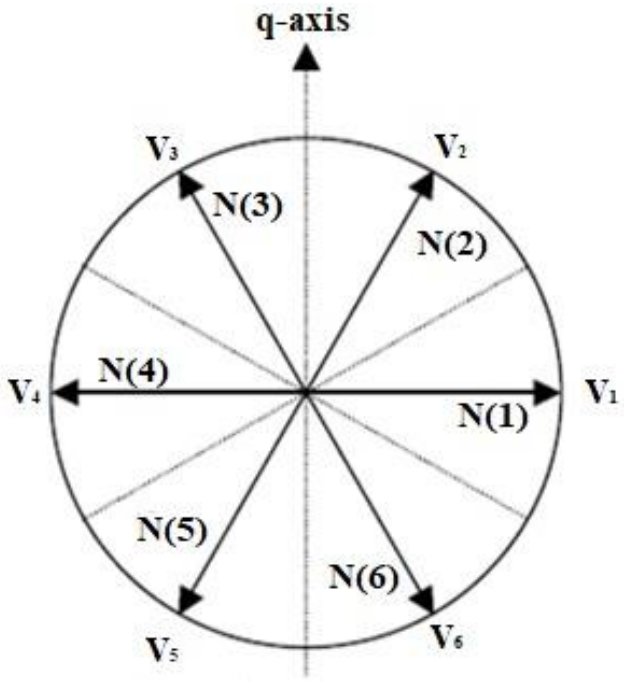

Figure 4.2 Voltage vectors and the six sectors for stator flux

So, in motoring mode, an angle is created between the stator flux and rotor magnetic flux this angle is called load angle δ.

Now if we divide the stator flux vector into d-q components we can write:

$$\psi_d^s = |\psi^s| \cos\delta \tag{4.2}$$

$$\psi_q^s = |\psi^s| \sin\delta \tag{4.3}$$

So, equation (2.16) can be re-written as,

$$i_d = \frac{|\psi^s| \cos\delta - \psi_r}{L_d} \tag{4.4}$$

$$i_q = \frac{|\psi^s| \sin\delta}{L_q} \tag{4.5}$$

According to (2.29), (4.4) and (4.5), we can say,

$$T_e = \frac{3}{2} P \left[\psi_r . \frac{|\psi^s| \sin\delta}{L_q} + \left(L_d - L_q\right) . \frac{|\psi^s| \cos\delta - \psi_r}{L_d} . \frac{|\psi^s| \sin\delta}{L_q}\right] \tag{4.6}$$

Now, For an SPM (Surface Mounted Machine) with a consistent air gap $L_q = L_d = L_s$. So, equation (4.6) becomes

$$T_e = \frac{3}{2} . \frac{P}{L_q} . |\psi^s| . \psi_r . \sin \delta \tag{4.7}$$

The torque increment equation can be written as

$$\Delta T_e = \frac{3}{2} . \frac{P}{L_q} . \psi_r |\psi^s| \Delta\delta . \sin \Delta\delta \tag{4.8}$$

From (4.7) and (4.8), we can see that the electromagnetic torque in a PMSM depends on the load angle (δ) and the strength of the stator flux (ψ^s). As a result, stator flux may be used to adjust load angle as much as necessary to provide a quick torque response. By selecting the proper switching of the inverter, we can adjust the stator flux magnitude and the load angle [33]. In figure 4.3 a representation of stator and rotor flux in the d-q reference frame is shown.

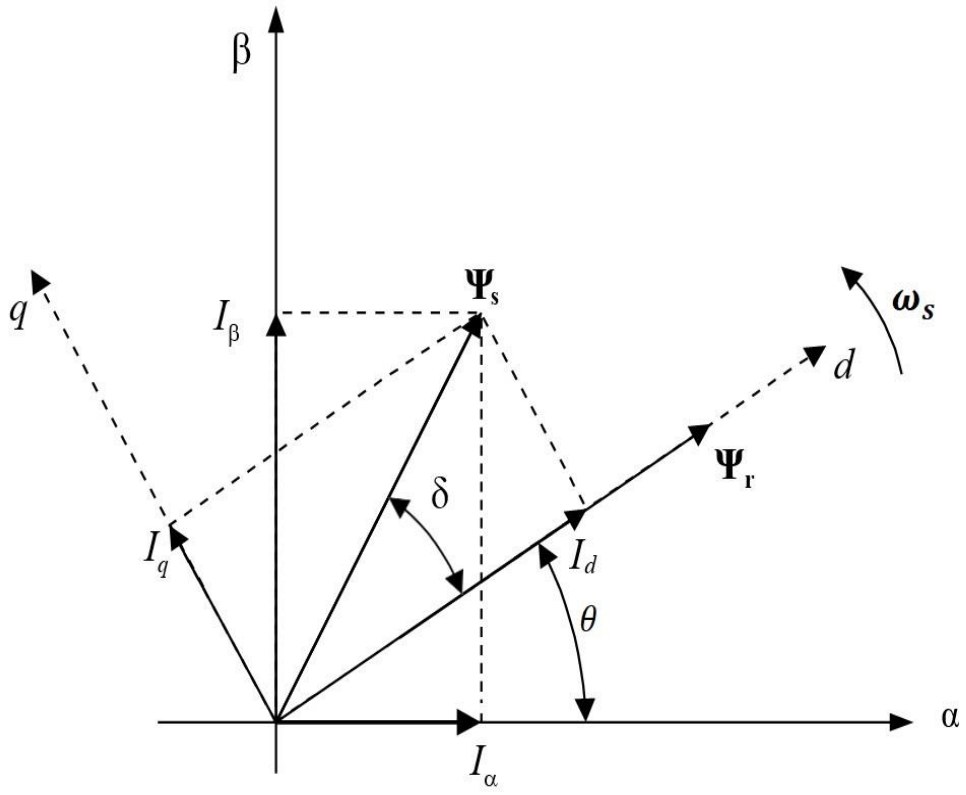

Figure 4.3 Stator and rotor flux in D-Q reference frame

4.3 Controller of DTC

A voltage vector is selected in DTC depending on the magnitude of the torque error, flux error, and the position of the sector in question. In this method, the active vector and the zero vector are employed at the same time in each sampling period.

4.3.1 Flux and sector estimator

We require the coordinate transformation in this torque control system as the currents from the three-phase motor are sampled. Three phase voltages ($v_a,\ v_b,\ v_c$) and currents ($i_a,\ i_b,\ i_c$) of the inverter are converted to αβ axis voltages (v_α,v_β) and currents (i_α,i_β) by using the Clarke transformation shown below. The relationship is demonstrated by the (4.9) and (4.10) functions.

$$\begin{bmatrix} i_\alpha \\ i_\beta \end{bmatrix} = \begin{bmatrix} 1 & -0.5 & -0.5 \\ 0 & \frac{\sqrt{3}}{2} & -\frac{\sqrt{3}}{2} \end{bmatrix} \begin{bmatrix} i_a \\ i_b \\ i_c \end{bmatrix} \tag{4.9}$$

$$\begin{bmatrix} v_\alpha \\ v_\beta \end{bmatrix} = \begin{bmatrix} 1 & -0.5 & -0.5 \\ 0 & \frac{\sqrt{3}}{2} & -\frac{\sqrt{3}}{2} \end{bmatrix} \begin{bmatrix} v_a \\ v_b \\ v_c \end{bmatrix} \tag{4.10}$$

A PMSM's stator flux linkage may be described in a stationary reference frame. According to Equation (2.11):

$$v_s = R_s.i_s + \frac{d\Psi_s}{dt} \tag{4.11}$$

$$\frac{d\Psi_s}{dt} = v_s - R_s.i_s \tag{4.12}$$

$$\Psi_s = \int (v_s - R_s.i_s)\, dt \tag{4.13}$$

It can be represented in the αβ axis using the following equations:

$$\psi_\alpha^s = \int (v_\alpha - R_s.i_\alpha) dt \tag{4.14}$$

$$\psi_\beta^s = \int \left(v_\beta - R_s.i_\beta\right) dt \tag{4.15}$$

Now, the stator flux can be calculated using ψ_α^s and ψ_β^s.

$$|\psi^s| = \sqrt{(\psi_\alpha^s)^2 + (\psi_\beta^s)^2} \tag{4.16}$$

The angle between two components of stator flux vector is defined using the following equation:

$$\alpha = \angle\psi^s = \tan^{-1}(\frac{\psi_\beta^s}{\psi_\alpha^s}) \tag{4.17}$$

According to the angle α the sector of the flux vector is estimated using the following table

Sector	Angle
1	[-30, 30]
2	[30, 90]
3	[90, 150]
4	[150, 210]
5	[210, 270]
6	[270, 330]

Table 4.1 Sector selection table

4.3.2 Torque estimation:

According to equation (2.28), the Electromagnetic torque can be estimated on the αβ axis.

$$T_e = \frac{3}{2}.P.\left(\psi_\alpha^s.i_\beta - \psi_\beta^s.i_\alpha\right) \tag{4.18}$$

4.3.3 Flux and torque hysteresis controller

For the DTC of a PMS motor, two hysteresis controllers are required. PMSM drive performance is affected by the ripple in torque and flux, the current harmonics, and the switching speed of power electronics devices. Torque hysteresis bands minimize torque ripple, whereas flux hysteresis bands reduce current distortion. Every sampling time, the inverter's switching status is updated. The inverter state remains fixed until the hysteresis controller output states change within a sampling interval. If the hysteresis band remains constant, the switching frequency is entirely determined by the rate of change of torque and flux.

4.3.3.1 Flux hysteresis controller

The flux error is calculated by comparing the flux reference point with the estimated flux ($\psi_{ref} - \psi^s = \psi_{err}$). If this mistake exceeds the hysteresis band limit, the flux controller output is high "1." If the mistake is inside the hysteresis range, the output is a low "0," as shown in Figure (4.4). If the output is high, it indicates that a flux increase is necessary, whereas a low output indicates that a flux drop is required. The flux controller's bandwidth is $2H_\psi$ [34].

The output signal of the hysteresis flux controller is defined as given below:

$$d\psi_s = \begin{cases} 1, & \psi_s < \psi_{ref} - H_\psi \\ 0, & \psi_s < \psi_{ref} + H_\psi \end{cases} \tag{4.20}$$

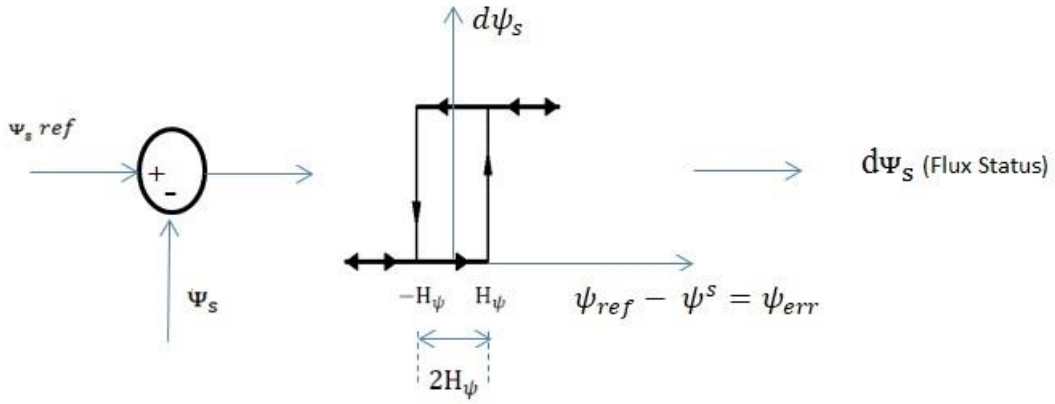

Figure 4.4 The flux comparator

4.3.3.2 Torque hysteresis controller

The torque error is calculated by comparing the torque reference point with the estimated torque ($T_{ref} - T_e = T_{err}$). It is necessary to either raise, reduce, or keep the torque constant.

Therefore, as illustrated in Figure (4.5), a three-level comparator is appropriate for torque demands. The torque status may be equal to "1," which indicates that an increase in torque is required; "-1," which indicates that a drop in torque is required; or "0," which indicates that no change in torque is necessary. The torque comparator's bandwidth is $2\mathrm{H}_T$ [34].

The output signal of the hysteresis torque controller is defined as given below:

$$dT_e = \begin{cases} 1, & T_e < T_{ref} - \mathrm{H}_T \\ 0, & T_e = T_{ref} \\ -1, & T_e < T_{ref} + \mathrm{H}_T \end{cases} \tag{4.21}$$

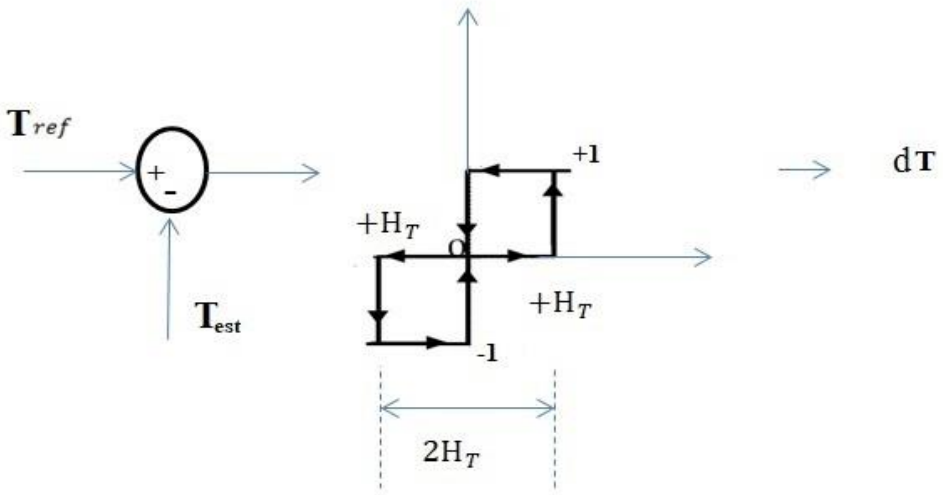

Figure 4.5 The torque comparator

4.3.4 Switching table

By selecting the best Voltage Source Inverter state, the necessary stator flux can be imposed. The stator voltage directly impresses the stator flux according to the following equation if the ohmic drops are disregarded for simplicity.

$$\frac{d\Psi_s}{dt} = v_s$$

$$or,\ \Delta\Psi_s = v_s \Delta t \tag{4.22}$$

By modifying the radial and tangential components of the stator flux-linkage space vector at its point, the stator flux modulus and torque may be independently controlled. There is a straight correlation between the two components of the same voltage space vector (R = 0). There are many possible dynamic stator flow locations shown in Figure (4.6), each with its own set of VSI states. The discontinuous line denotes six sectors of the possible global location.

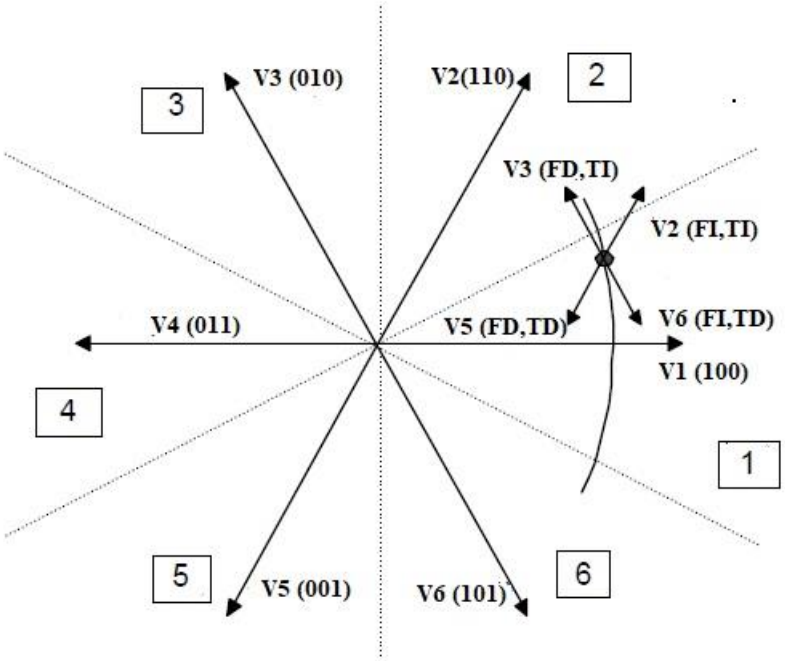

Figure 4.6 Different potential switching voltage vectors and the location of the stator flux vector.

Figure 4.6 shows how the general Table 4.2 can be written. Table 4.2 demonstrates that the states V_n and V_{n+3}, which, depending on where the stator flux is, can both increase (first 30 degrees) and decrease (second 30 degrees) torque in the same sector, are not properly considered when calculating torque.

VOLTAGE VECTOR	INCREASE	DECREASE
Stator Flux	V_n, V_{n+1}, V_{n-1}	$V_{n+2}, V_{n+3}, V_{n-2}$
Torque	V_{n+1}, V_{k+2}	V_{n-2}, V_{n-1}

Table 4.2 General selection table for direct torque control, (n=sector)

Below is a DTC traditional lookup table:

The Output of hysteresis controllers		**Sector(N)**					
$d\psi_s$	dT_e	**N=1**	**N=2**	**N=3**	**N=4**	**N=5**	**N=6**
1	1	V_2	V_3	V_4	V_5	V_6	V_1
	0	V_7	V_0	V_7	V_0	V_7	V_0
	-1	V_6	V_1	V_2	V_3	V_4	V_5
0	1	V_3	V_4	V_5	V_6	V_1	V_2
	0	V_0	V_7	V_0	V_7	V_0	V_7
	-1	V_5	V_6	V_1	V_2	V_3	V_4

Table 4.3 Voltage vector selection table for direct torque control

Sectors S1 through S6 make up the stator flux space vector. There are only two possible values for the stator flux modulus error following the hysteresis block (Figure 4.4). Three alternative values can be assigned to the torque error following the hysteresis block (Figure 4.5). When the torque error is within the specified hysteresis limits, the zero voltage vectors V0 and V7 are chosen and must not vary [35].

4.4 DTC Schematic

Figure 4.7 depicts a potential Direct Torque Control scheme. As seen, there are two distinct loops that correlate to the stator flux's magnitudes plus torque. The reference value of torque is calculated using a PI controller. The input of the PI controller is speed error and the output is

the torque reference. The error values are delivered to the two-level and three-level hysteresis blocks, respectively, based on comparisons between the reference and actual values for the flux stator modulus and torque. As inputs to the look-up table are the outputs of the stator flux error and torque error hysteresis blocks, as well as the location of the stator flux (see table 4.3). The flux position of the stator is divided into six discrete sectors. The stator flux modulus and torque errors tend to be restricted inside their respective hysteresis bands, as seen in Figure 4.7. Figure 4.8 diagram shows how to do the DTC flux and torque calculations using two distinct phases currents and the PMSM input voltage [35].

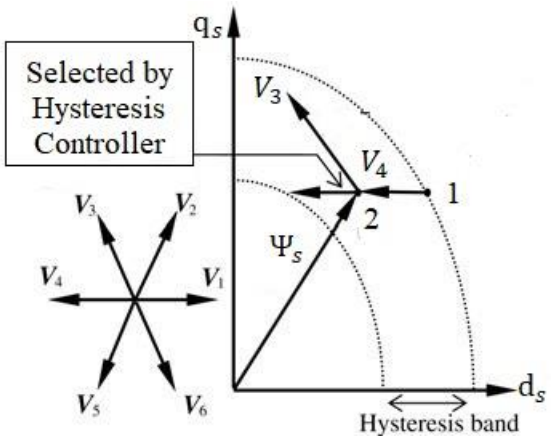

Figure 4.7 Potential stator flux vector paths with DTC inside the hysteresis band

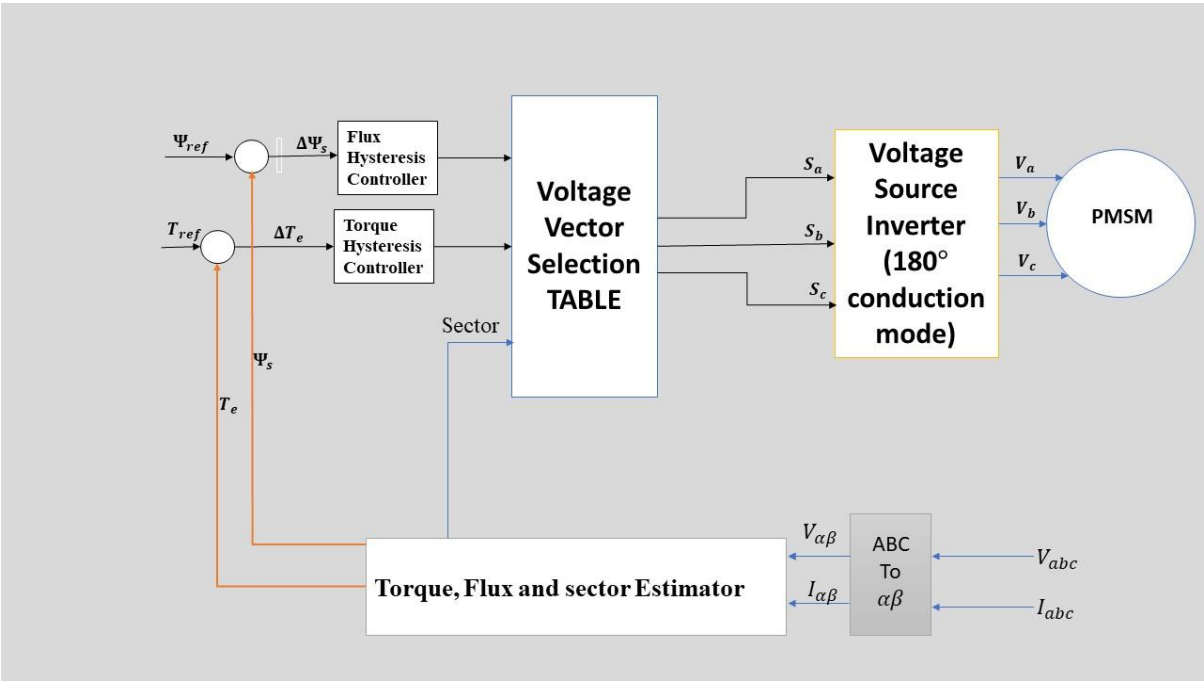

Figure 4.8 Schematic diagram of DTC

Chapter 5

Duty Ratio Modulation

5.1 Introduction

The conventional DTC induction motor drive has torque and flux ripples because none of the inverter vectors can give the right changes in both torque and stator flux. However, the ripples in the electromagnetic torque and stator flux may be decreased utilising several ways. Some of these strategies require high switching frequencies or a change in the topology of the inverter. However, it is possible to use systems that don't need any of these strategies, like duty ratio control.

5.2 Reason of Use

Increasing the switching frequency is beneficial in the DTC PMSM drive. Because it decreases the harmonic content of stator currents and also leads to reduced torque ripple. But, using a high switching frequency will result in an increase in switching losses which leads to a reduction in efficiency. It will also raise the stress on the inverter's semiconductor components. Besides this, a fast processor is necessary when the switching frequency is high since the control processing time becomes shorter. This raises the cost. Also, it is feasible to employ more switches when the inverter topology is modified, however, this will also raise the prices. So, to counter those drawbacks duty ratio control strategy is used which does not require an inverter which has a higher number of switches.

5.3 Application

Since the stator current and electromagnetic torque exceed their reference values early in the cycle when a voltage vector is used in a typical DTC PMSM drive, a considerable torque ripple is produced throughout the cycle. The zero switching vectors are then applied to lower the electromagnetic torque to the reference value, which is followed by switching cycles. The proposed procedure includes applying the specified active states to the inverter for only long enough to obtain the torque and flux reference values. When switching is complete, a null state is chosen that will not nearly modify the torque or flux. As a result, each time a switch is made,

a duty ratio must be calculated. It is feasible to apply any voltage to the motor by changing the duty ratio between its extreme extremes [35].

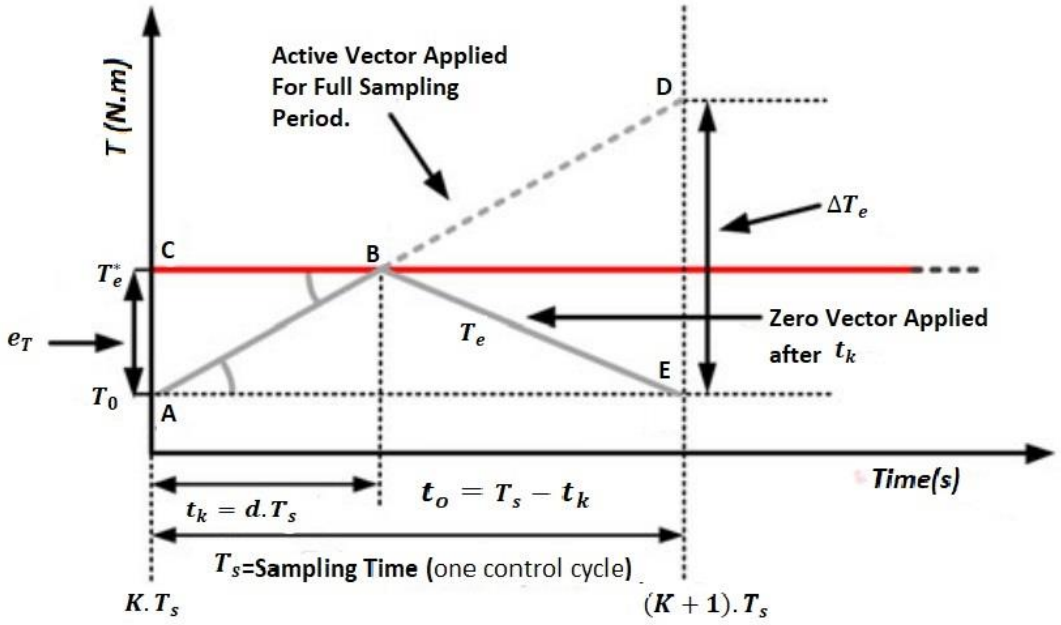

Figure 5.1 Duty ratio modulation

5.4 Duty Ratio Calculation

The main task for duty ratio modulation is to define the duty ratio. The total sample period of the voltage vector is divided into two parts. The duration of active voltage vector switching $\boldsymbol{t_k}$ and the switching time of zero voltage vector $\boldsymbol{t_0}$. The duty ratio calculation block is used to compute these. The torque error has a direct correlation with the on-time $\boldsymbol{t_k}$**.** The on-time is calculated using the following equation [20].

$$t_k = \begin{cases} \frac{\Delta T_m}{T_H} T_s; & \Delta T_m < T_H \\ T_s; & \Delta T_m > T_H \end{cases} \tag{5.1}$$

Off time, $\boldsymbol{t_0} = T_s - t_k$.

While maintaining the simplicity of traditional DTC, this method can significantly reduce torque ripple while maintaining a constant switching frequency. This is the main advantage of this duty ratio control method.

The switching signal comparison between the traditional method and the suggested one is shown in Fig. 5.2. In the traditional approach, each sampling period only uses one switching vector. However, as depicted in Fig. 5.1 (a), the proposed method makes use of the effective voltage vector and zero-vector 5.1 (b). The torque waveform in the suggested control scheme is shown in Fig. 5.1 (c). Effective voltage vector and zero-vector are provided during a sampling period for comparison with the traditional DTC [20].

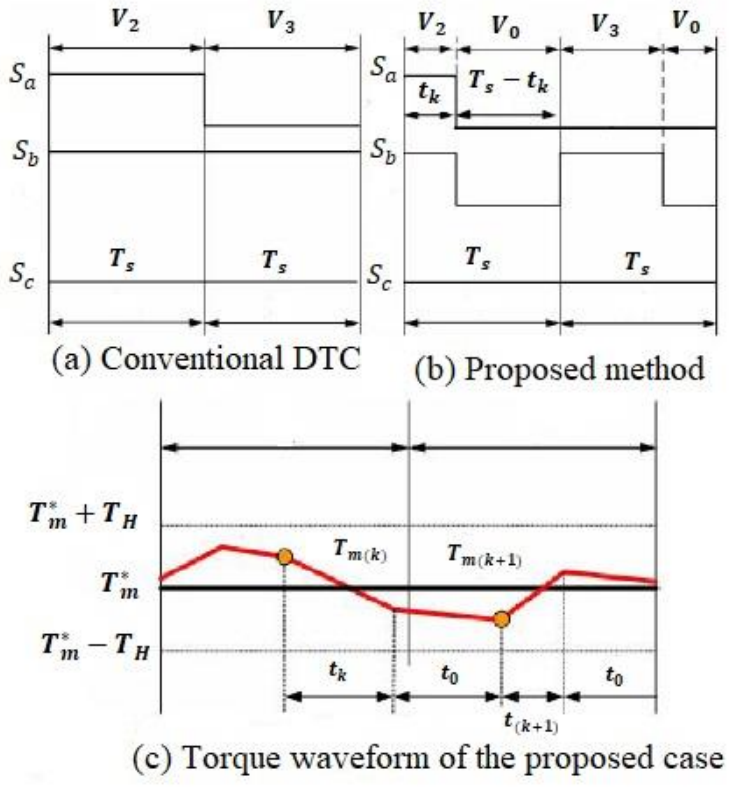

Figure 5.2 The comparisons of switching signals and torque waveform

5.5 Duty Ratio Calculation Without Torque Hysteresis Band

But for the method mentioned above, the duty ratio depends on how wide the torque hysteresis band is. If the torque hysteresis bandwidth is narrower, the amount of ripple will be less. If the width is so big, there are also a lot of waves. This indicates that the hysteresis bandwidth affects the ripple content. The aforementioned technique has been modified to reduce torque ripple no matter how wide the hysteresis band is. Here, the duty ratio is determined solely by the torque error; (width of the hysteresis band is not taken into consideration) [21].

$$d = \frac{\Delta T_m}{C} \tag{5.2}$$

The new on-time is calculated using this duty ratio.

$$t_k = \begin{cases} d.T_s; & \Delta T_m < T_H \\ T_s; & \Delta T_m > T_H \end{cases} \tag{5.3}$$

Where C is a fixed value. The ripple content is also small due to the low value of C. When C is high, there is a greater amount of ripple content.

Active vector is applied during the switching time (t_k) and zero vector is applied during the off time. With constant switching frequency, torque ripple can be significantly reduced. By raising the switching frequency, torque ripple can be even more significantly reduced [21].

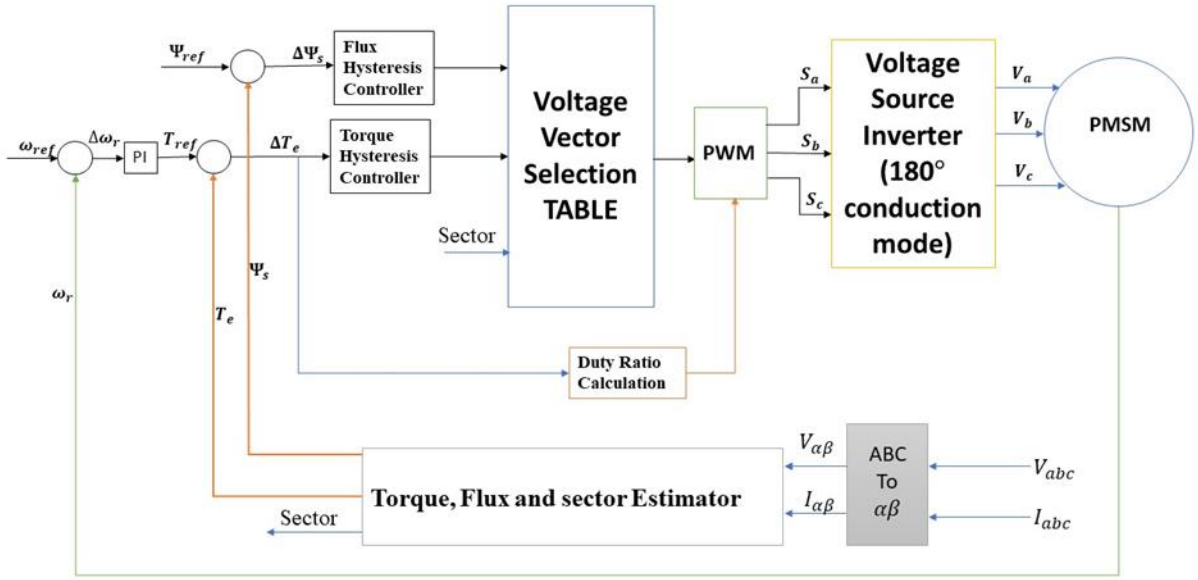

Figure 5.3 Duty ratio modulated direct torque control

Figure 5.3 demonstrates the block diagram for Modified DTC of the PMSM. The only difference between this method and conventional DTC is the addition of a block for duty ratio calculation. Only the voltage vector is determined by the switching table. The voltage vector and switching time are used to create the final switching pulses. The on-time t_k is calculated by the duty ratio calculation block. Then switching pulses are generated using the on time. A PWM block is used in order to modulate the voltage vector which is coming from the Voltage Vector selection Table [21].

Chapter 6

Maximum Torque Per Ampere Scheme

6.1 Basic Principle Of MTPA

Maximizing torque while using the least amount of stator current is the purpose of the MTPA scheme. Overall system efficiency rises due to reducing copper loss in this way—at least while copper loss is noticeable. [36].

6.1.1 Field weakening control

The stator voltages, rated current, and back emf regulate the maximum speed of a motor when vector control is used to operate it at rated flux. This is referred to as the base speed. Beyond this speed, the machine's operation becomes complex because the back emf exceeds the supply voltage. However, if the D-axis stator current (I_d) is set to a negative value, the rotor flux linkage is reduced, allowing the motor to run faster than the base speed. This is known as field-weakening control of the motor [37].

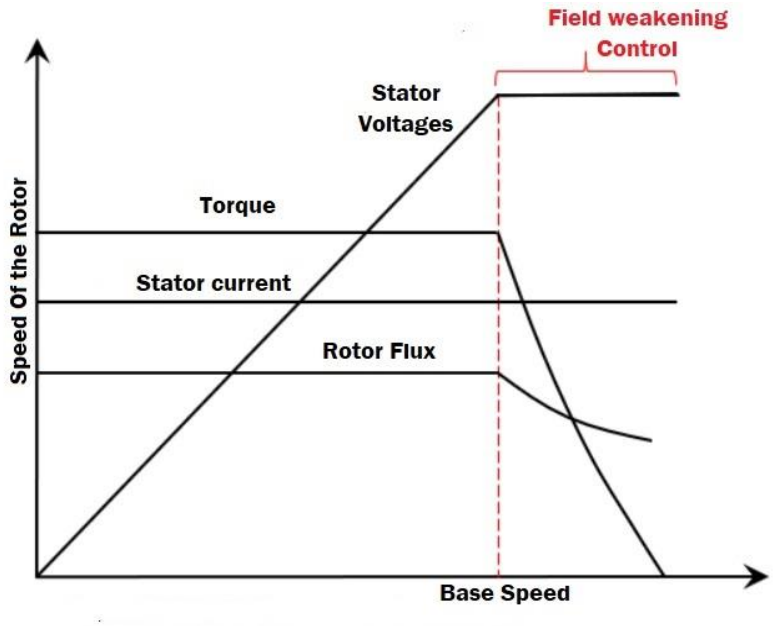

Figure 6.1 Field weakening control plot

The reference d-axis current (I_d) in the field-weakening control also, restricts the reference q-axis current (I_q), and hence the torque output, depending on the connected load and rated current of the machine. As a result, the motor functions in the constant torque region until it reaches the base speed. As shown in Figure 6.1, it functions in the constant power region with a restricted torque above the base speed [37].

6.1.2 MTPA

The saliency in the magnetic circuit of the rotor leads to a higher L_q/L_d ratio for the inner PMSMs (greater than 1). This results in rotor reluctance torque (in addition to the existing electromagnetic torque). As a result, you can operate the machine at an optimal combination of i_d and i_q to generate more torque for the same stator current,

$$i_m = \sqrt{(i_d)^2 + \left(i_q\right)^2} \tag{6.1}$$

Because the stator current losses are reduced, the machine becomes more efficient. Maximum Torque Per Ampere (MTPA) is the name of the algorithm which is used to create the reference "i_d" and "i_q" currents for the machine's maximum torque output [38].

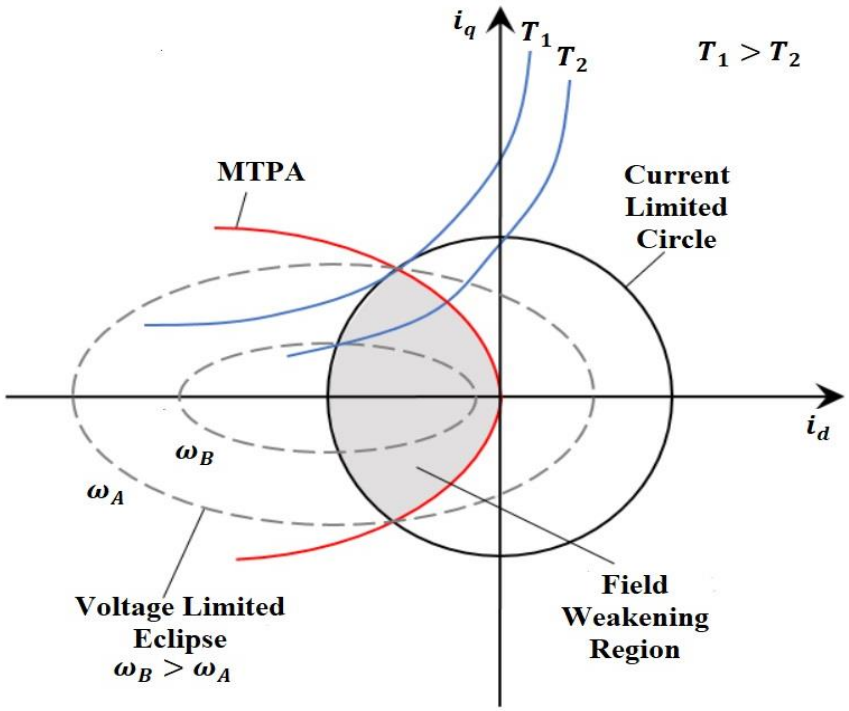

Figure 6.2 MTPA curve

6.2 Control Action

The d-q currents are specifically specified when employing the maximum torque per ampere (MTPA) scheme method by,

$$i_{d,MTPA} = f_d(T^*) \text{ and } i_{q,MTPA}=f_q(T^*) \tag{6.2}$$

The optimal current $i_{d,MTPA}$ and $i_{q,MTPA}$ is the function of optimal torque T^*.

D-Q axis flux vector can be obtained by equation (2.28)

$$\Psi_q = L_q . i_q \tag{6.3}$$

$$\Psi_d = L_d . i_d + \Psi_r \tag{6.4}$$

Because of this, an indirect technique to calculate the stator flux amplitude Ψ_S^* relative to dq currents $i_{d,MTPA}$, and $i_{q,MTPA}$ by,

$$\Psi_s^* = \sqrt{\left(L_d . i_{d,MTPA} + \Psi_r\right)^2 + (L_q . i_{q,MTPA})^2} \tag{6.5}$$

The d-q axis currents in the MTPA scheme are often determined from a LUT or by calculating a series of equations online. In this thesis, the d-axis current is forced to zero in order to achieve MTPA.

If, $i_{d,MTPA} = 0$ then equation (6.1) becomes,

$$i_{MTPA} = i_{q,MTPA} \tag{6.6}$$

Also,

$$i_{MTPA} = \frac{2.T^*}{3.P.\Psi_r} \tag{6.7}$$

In equation (6.5) if we put $i_{d,MTPA} = 0$. It becomes,

$$\Psi_s^* = \sqrt{(\Psi_r)^2 + (L_q . i_{q,MTPA})^2} \tag{6.8}$$

Now, from equations (6.6), (6.7), and (6.8) we can establish a relationship between torque and flux by the following equation,

$$\Psi_s^* = \sqrt{{\Psi_r}^2 + {L_q}^2 \left(\frac{2.T^*}{3.P.\Psi_r}\right)^2} \tag{6.9}$$

Using this equation, we can establish a relationship between flux and torque.

Chapter 7

Modified Duty Ratio Modulation

7.1 Basic Idea

In this thesis, the MTPA approach and Duty Ratio Modulated DTC are combined. In order to get a better torque response. Using the MTPA equation, a relationship between torque and flux has been established, and the torque is calculated by converting the estimated flux. Following a comparison with the reference torque, a new torque error was generated, and it was used to calculate the duty ratio. The torque ripple is reduced using this technique.

7.2 Proposed Method

In equation (5.3). The duty ratio is calculated using torque error. $d = \frac{\Delta T_m}{C}$.

Previously the torque error was being calculated by comparing the estimated torque and the reference torque (output of PI controller).

$$\Delta T = T_{ref} - T_{est} \tag{7.1}$$

In this thesis, the torque is calculated from estimated flux using the MTPA equation and then it is compared with the reference torque (output of PI controller). In order to achieve a new value of ΔT.

From equation (6.9),

$$\Psi_s = \sqrt{{\Psi_r}^2 + {L_q}^2 \left(\frac{2T_{new}}{3.P.\Psi_r}\right)^2}$$

So,

$$T_{new} = \frac{3P.\Psi_r}{2L_q} \times \sqrt{|\Psi_s^2 - \Psi_r^2)|} \tag{7.2}$$

Using the above equation, the estimated flux is converted into corresponding torque and using this newly calculated torque we can calculate the new value of torque error.

$$\Delta T_{new} = T_{ref} - T_{new} \tag{7.3}$$

Now, using this new torque error value the new duty ratio is calculated.

$$d_{new} = \frac{\Delta T_{new}}{C} \tag{7.4}$$

By using this method, a significant reduction in torque ripple can be observed.

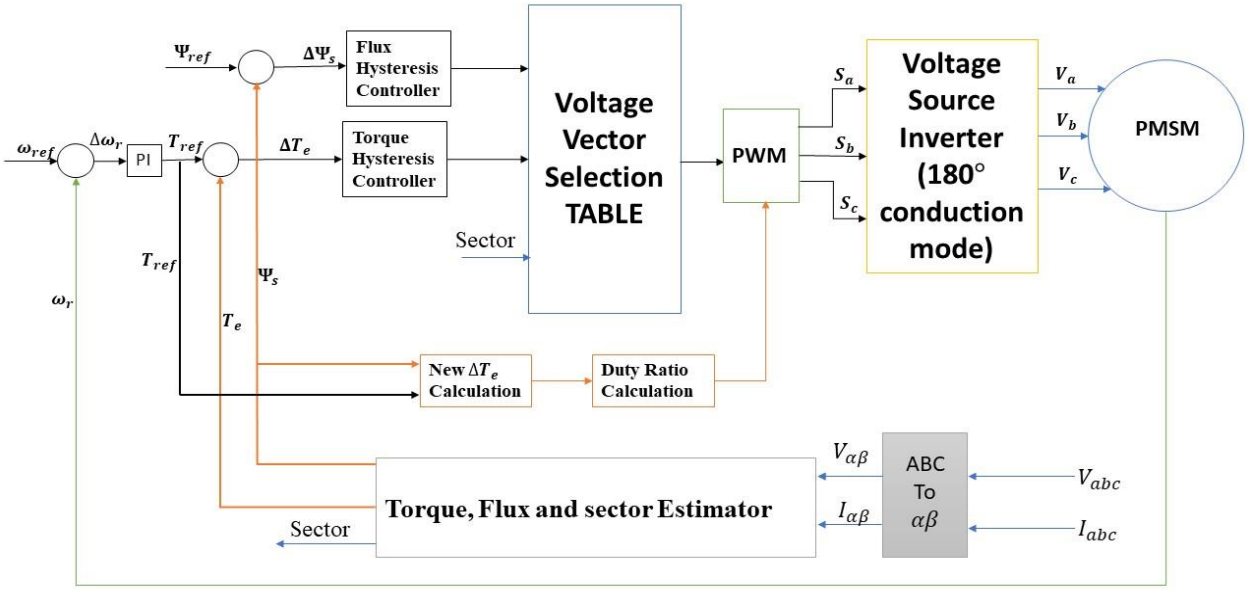

Figure 7.1 Schematic diagram of modified DTC

In Figure 7.1 a schematic diagram of the proposed method is shown. The comparison between the two methods and the results have been discussed in the next chapter.

Chapter 8

Results and Discussion

8.1 Simulation

Three types of simulation models have been tested and compared in this paper at first a model for conventional DTC is simulated in MATLAB Simulink. Then it is modified with the duty ratio modulation technique and the result of them is compared. After this, the duty ratio modulated DTC has again modified now the torque for torque error calculated by converting the estimated flux using the MTPA equation. The results from each Simulation are obtained from MATLAB Simulink and provided here. At first, the motor parameter used for simulation is provided here:

Parameters	**Values**	**Unit**
No. of Pole Pairs (P)	2	
Stator Resistance (R_s)	2.875	Ohm (Ω)
Permanent Magnet Flux (Ψ_r)	0.175	Weber (Wb)
Q-axis Inductance (L_q)	0.0085	Henry (H)
D-axis Inductance (L_d)	0.0085	Henry (H)
Moment of Inertia (J)	0.0008	Kg-m^2
Friction Factor (B)	0.0001	Nms

Table 8.1 PMSM parameters

8.1.1 Simulink block diagrams

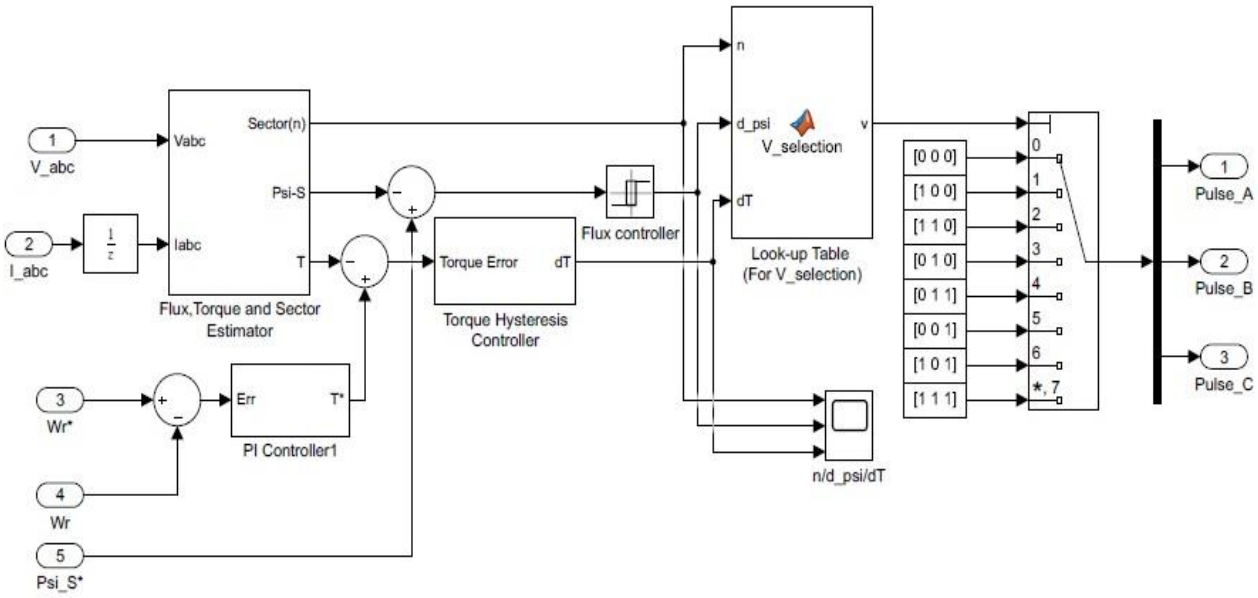

Figure 8.1 Simulink block diagram for conventional DTC of PMSM

In Figure 8.1 a Simulink block diagram for DTC is shown. Here estimation block is used to estimate Flux, Torque and Sector. Then the estimated values are compared with their reference values and an error is generated. Here, hysteresis comparators are used to regulate directly the torque and stator flux. Then using the output values of the hysteresis controllers and the estimated sector the proper switching voltage vector is selected from the vector selection table.

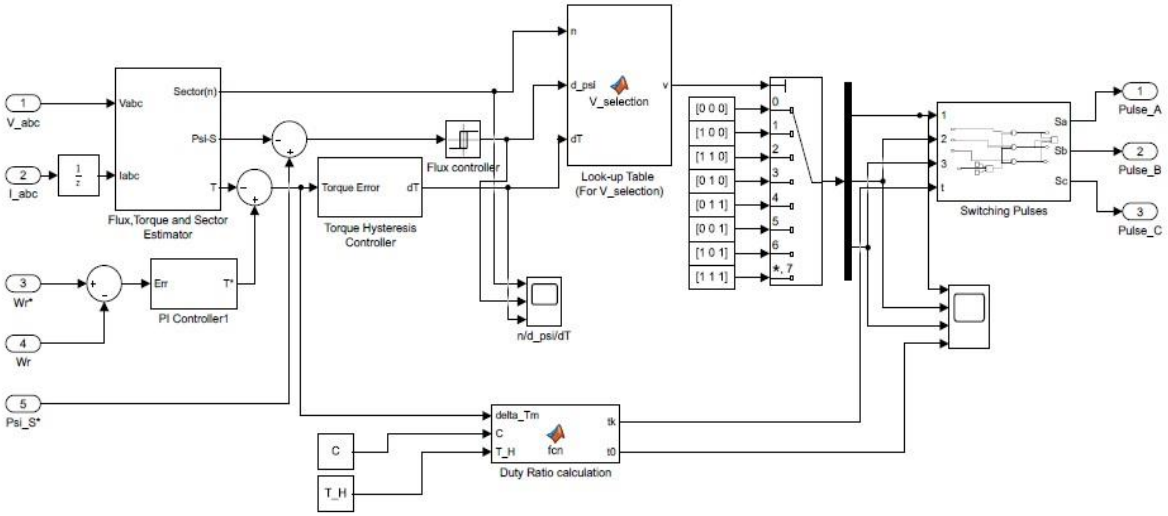

Figure 8.2 Simulink block diagram for duty ratio modulated DTC of PMSM

This block diagram in Figure 8.2 is very much similar to conventional DTC but here an extra block is used to calculate the duty ratio also a PWM block is used to modulate the switching pulses.

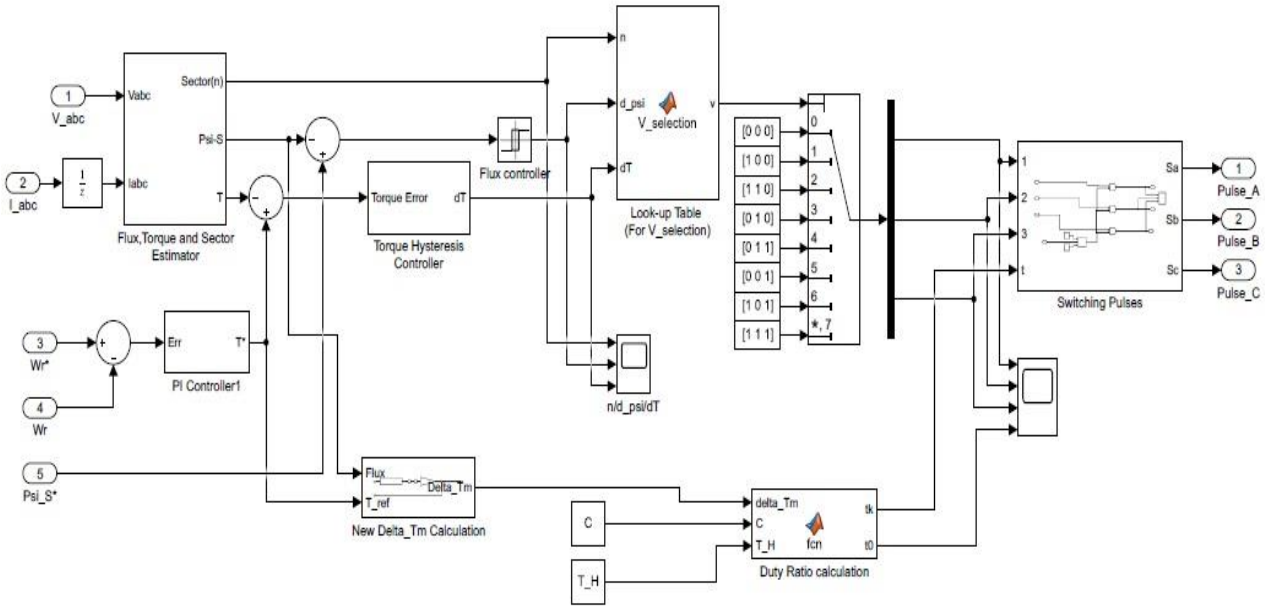

Figure 8.3 Simulink block diagram for modified duty ratio modulated DTC of PMSM

In this block diagram in Figure 8.3 ΔT_m for duty ratio control is calculated differently. Here the torque is calculated using flux with the help of the MTPA equation then it is compared with the reference value of torque.

8.2 Results

8.2.1 Speed response

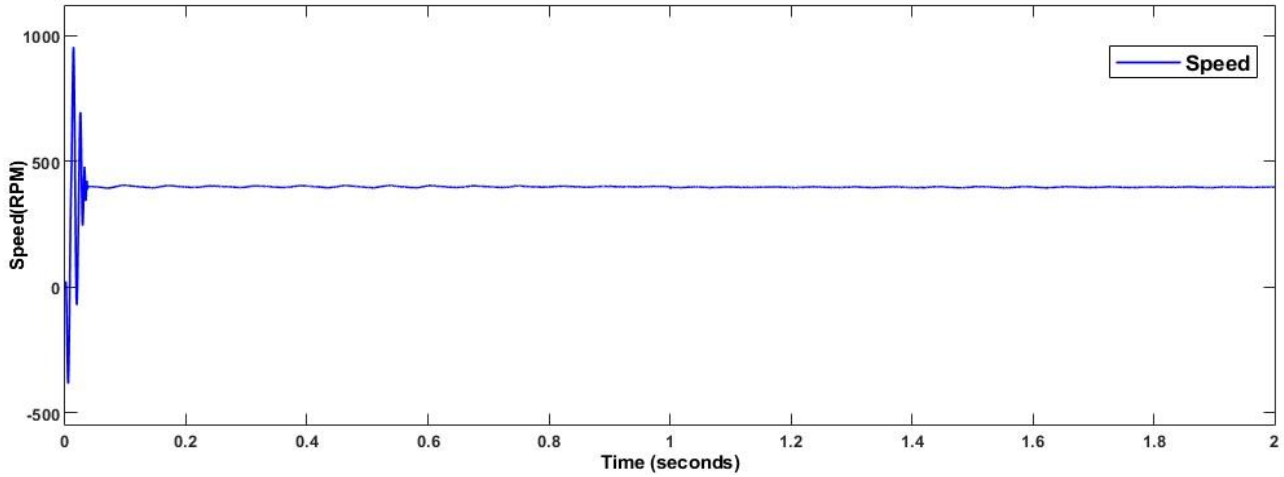

Figure 8.4 Simulation result of speed response using conventional-DTC

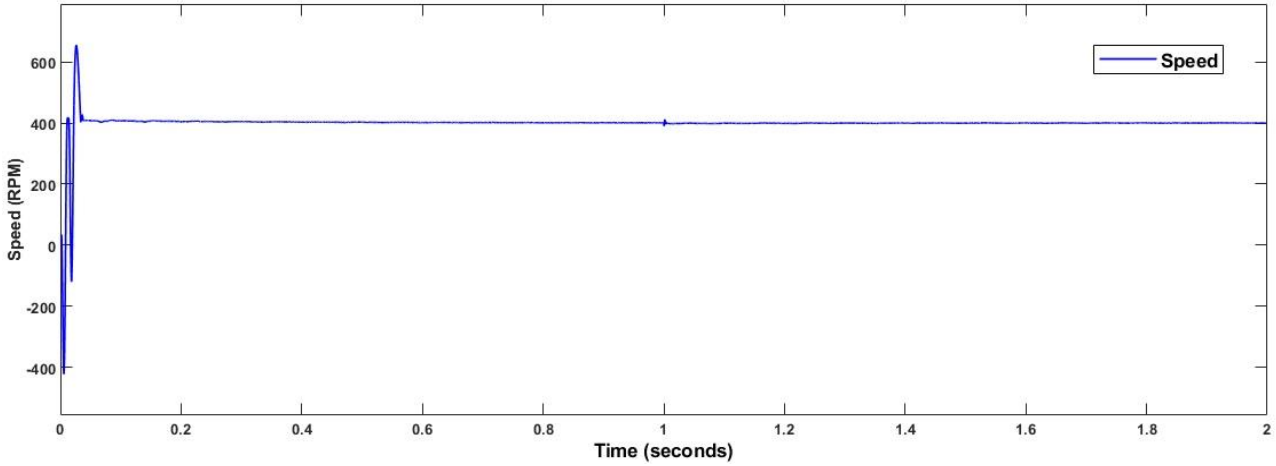

Figure 8.5 Simulation result of speed response using duty ratio modulated DTC

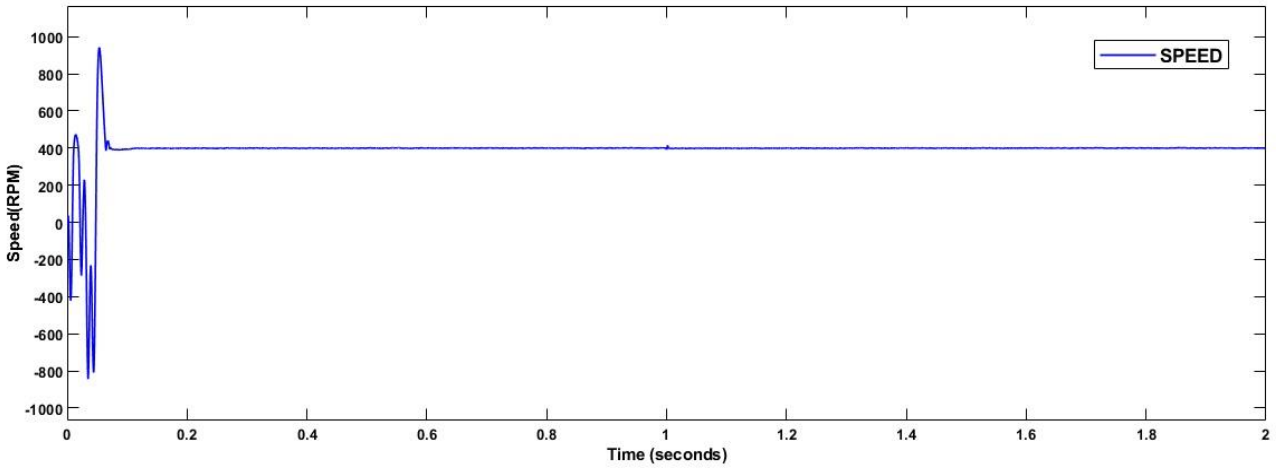

Figure 8.6 Simulation result of speed response using modified duty ratio modulated DTC

8.2.2 Torque response

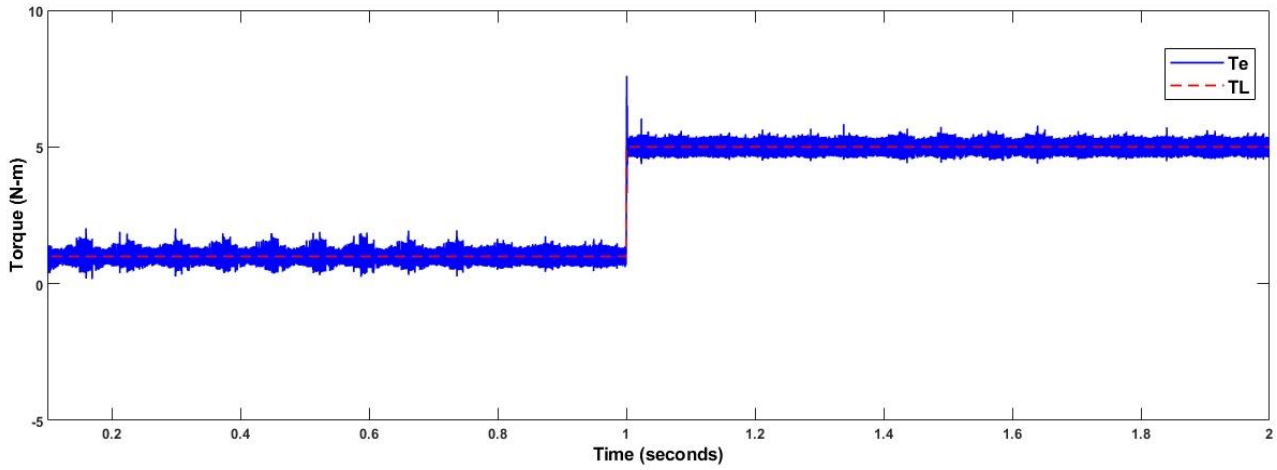

Figure 8.7 Simulation result of torque response using conventional-DTC

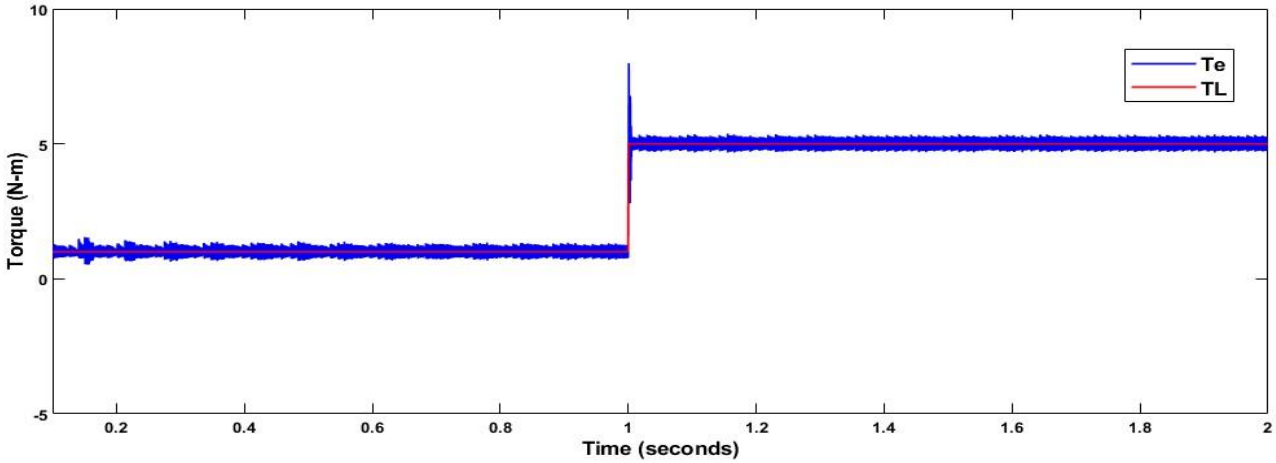

Figure 8.8 Simulation result of torque response using duty ratio modulated DTC

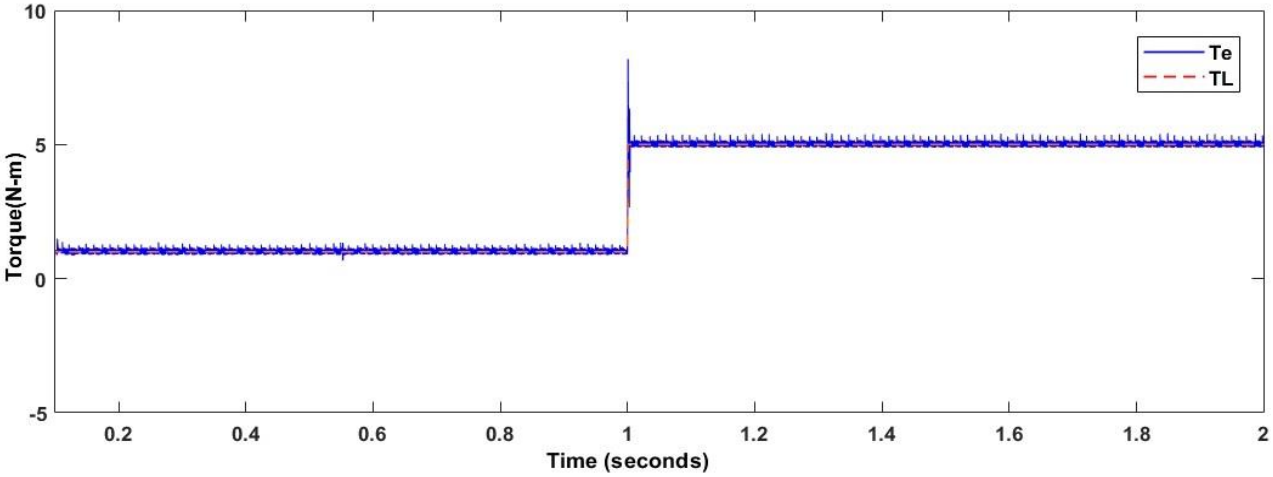

Figure 8.9 Simulation result of torque response using modified duty ratio modulated DTC

8.2.3 D-Axis current response

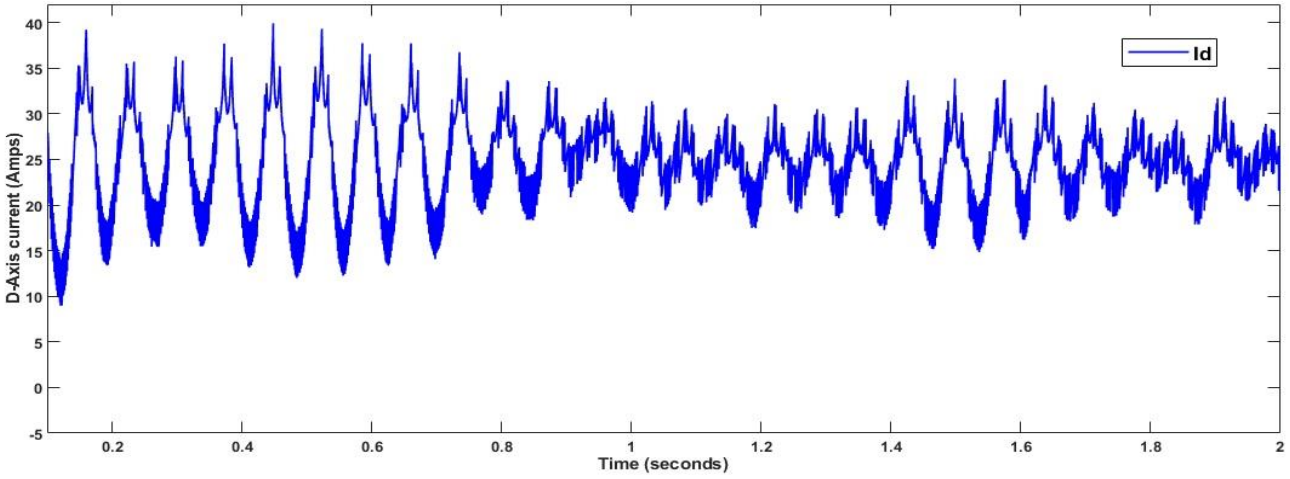

Figure 8.10 Simulation result of D-axis current using conventional-DTC

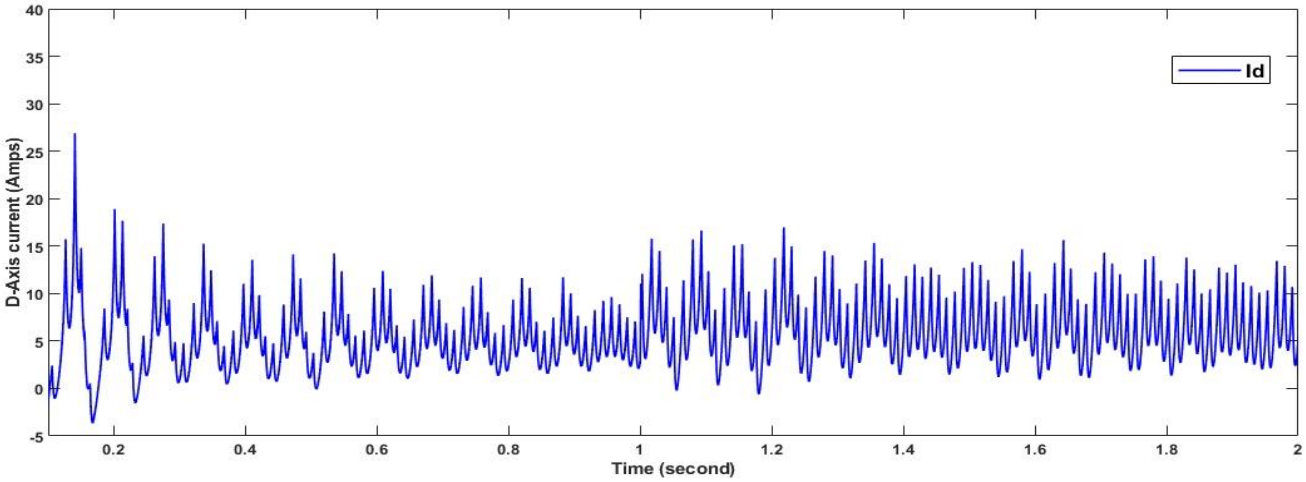

Figure 8.11 Simulation result of D-axis current using duty ratio modulated-DTC

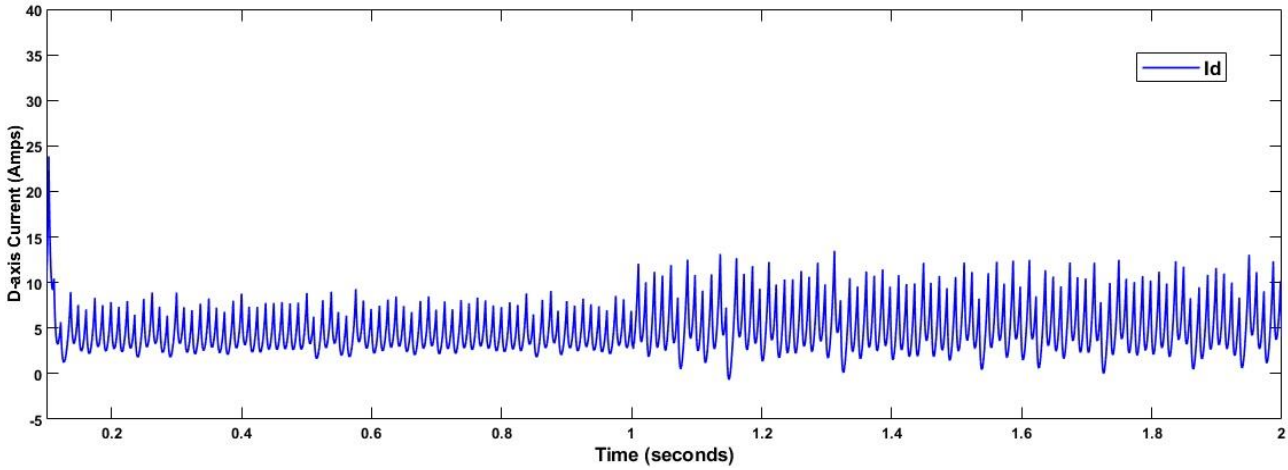

Figure 8.12 Simulation result of D-axis current using modified duty ratio modulated-DTC

8.2.4 Q-Axis current response

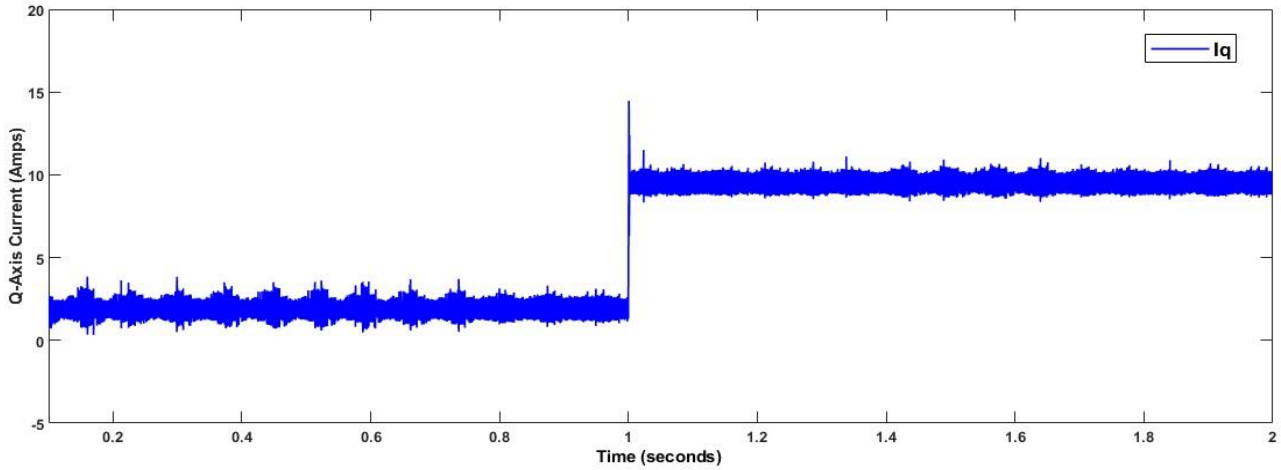

Figure 8.13 Simulation result of Q-axis current using conventional-DTC

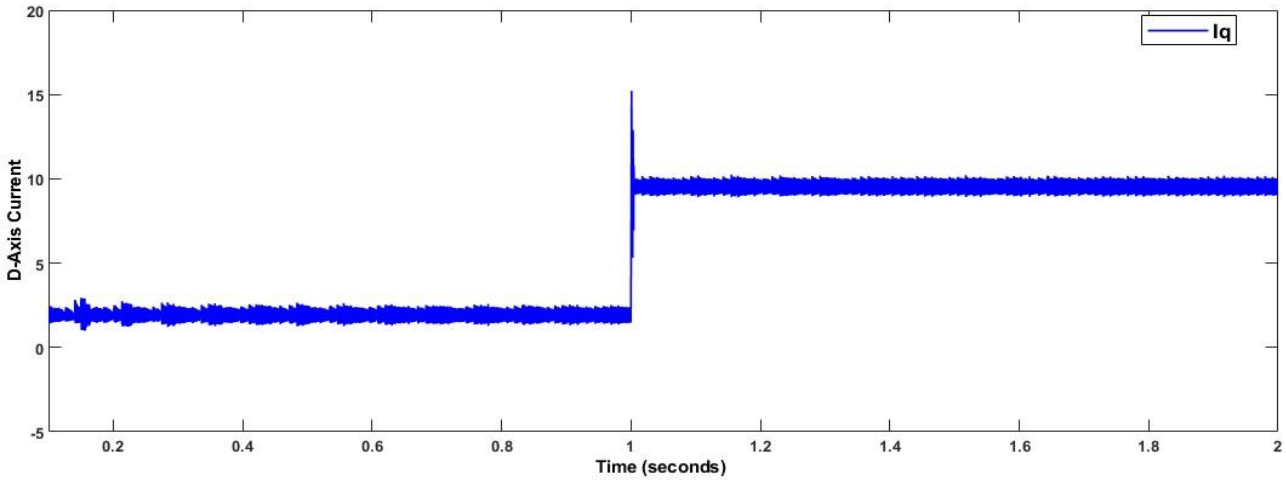

Figure 8.14 Simulation result of Q-axis current using duty ratio modulated-DTC

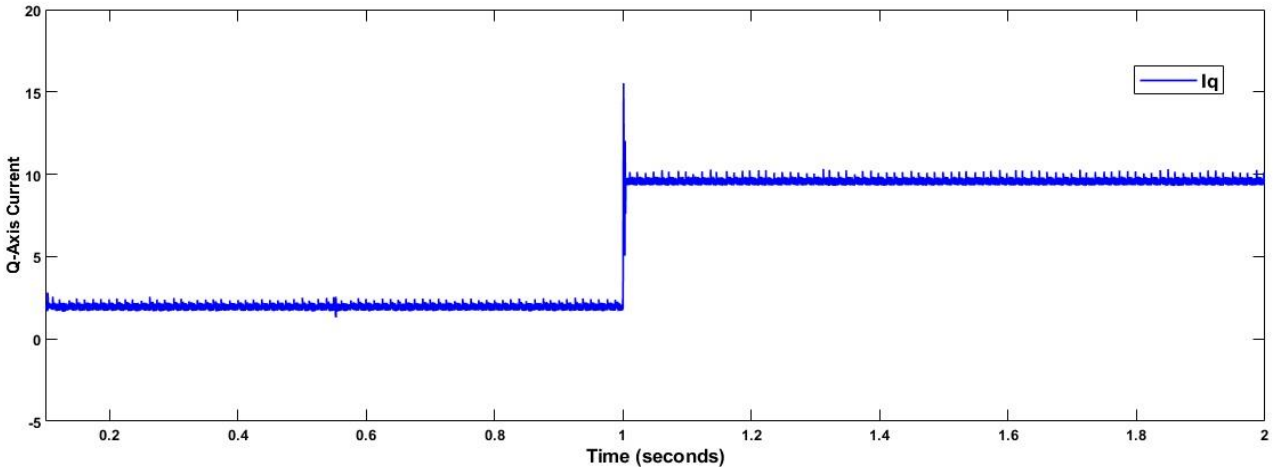

Figure 8.15 Simulation result of Q-axis current using modified duty ratio modulated -DTC

8.2.5 D-Axis voltage response

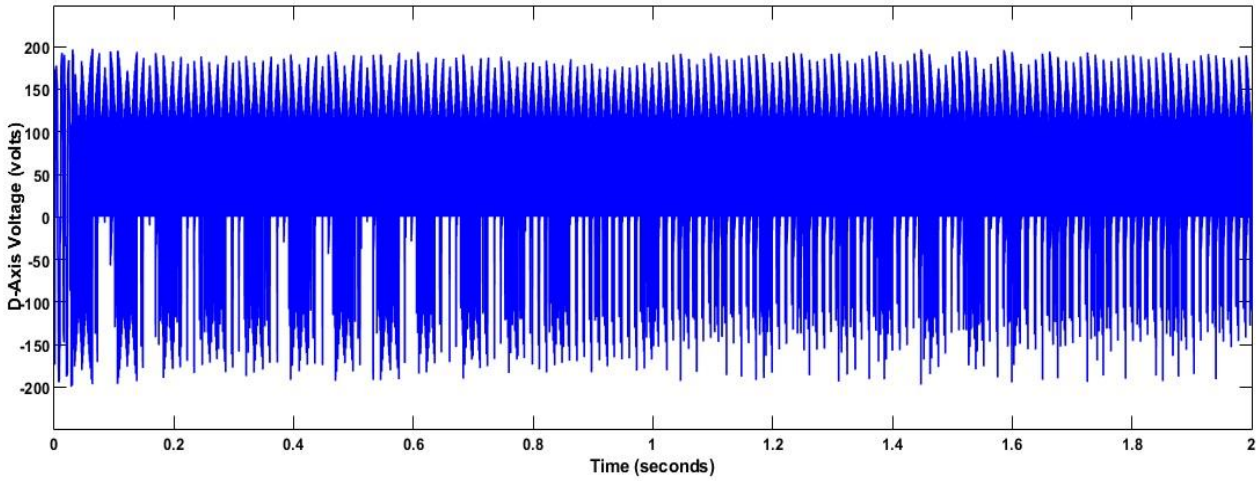

Figure 8.16 Simulation result of D-axis voltage using conventional-DTC

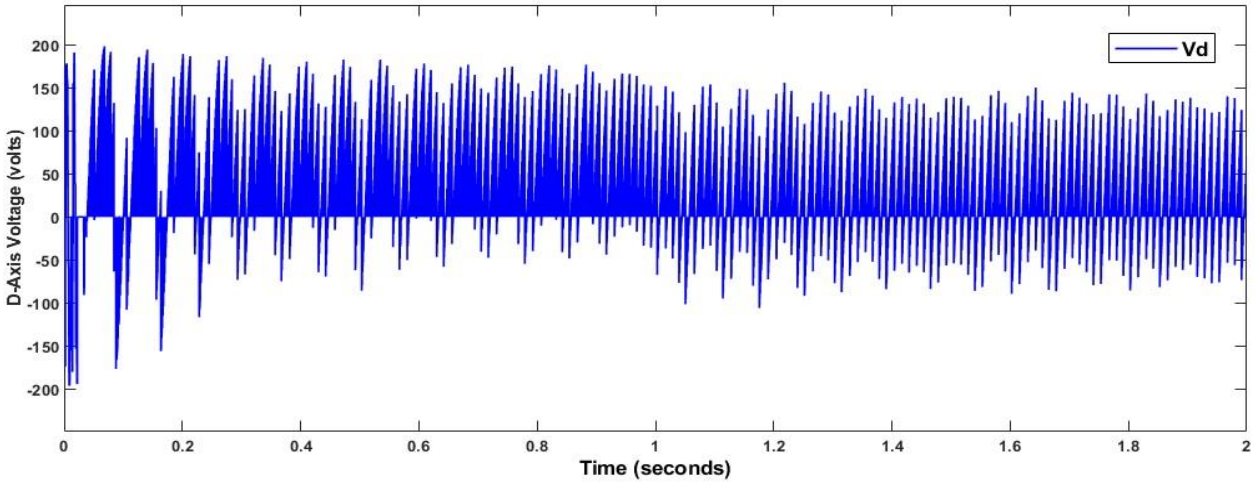

Figure 8.17 Simulation result of D-axis current using duty ratio modulated -DTC

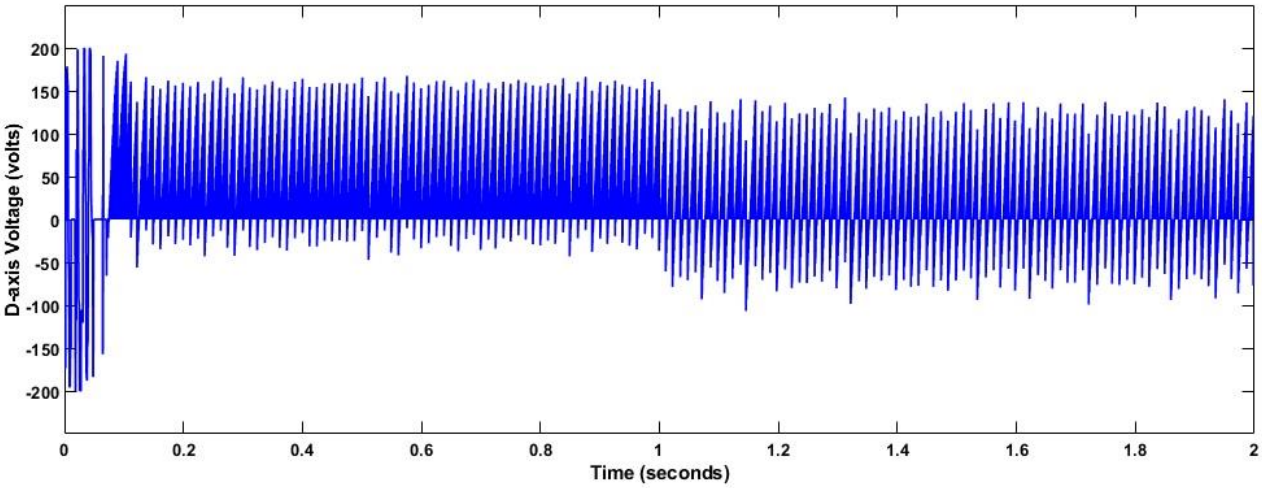

Figure 8.18 Simulation result of D-axis voltage using modified duty ratio modulated -DTC

8.2.6 Q-Axis voltage response

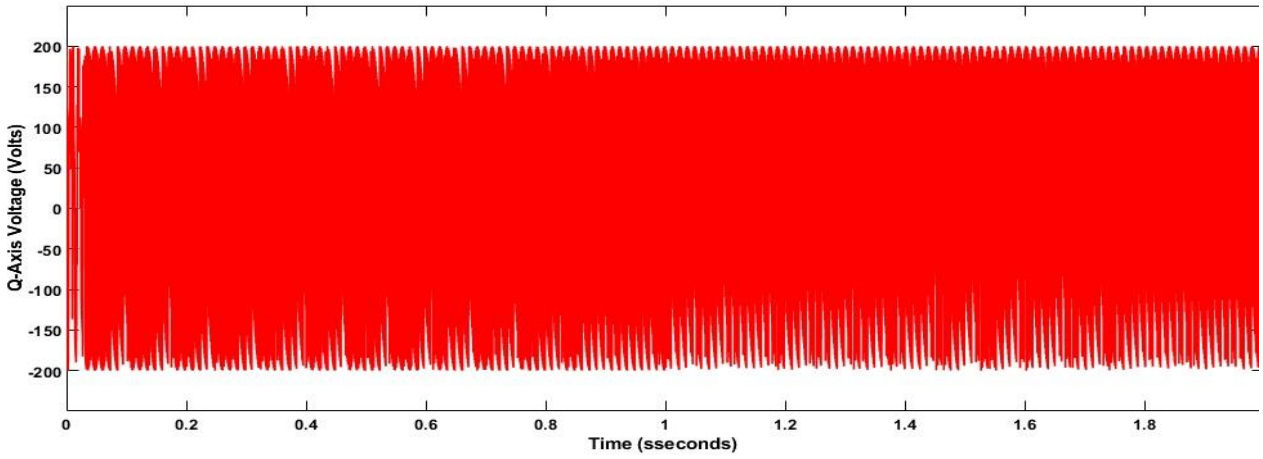

Figure 8.19 Simulation result of Q-axis voltage using conventional-DTC

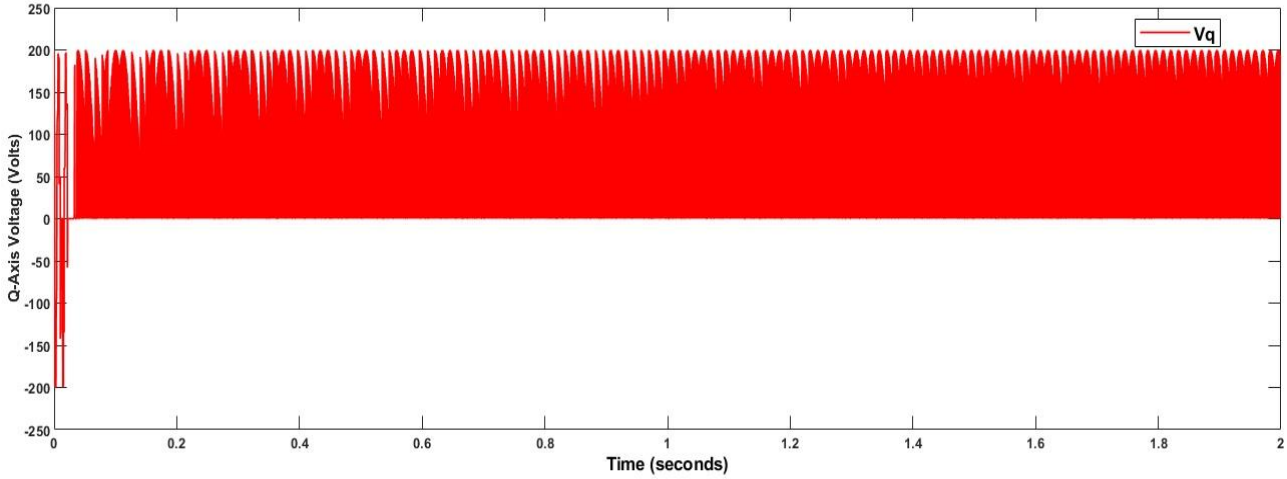

Figure 8.20 Simulation result of Q-axis voltage using duty ratio modulated -DTC

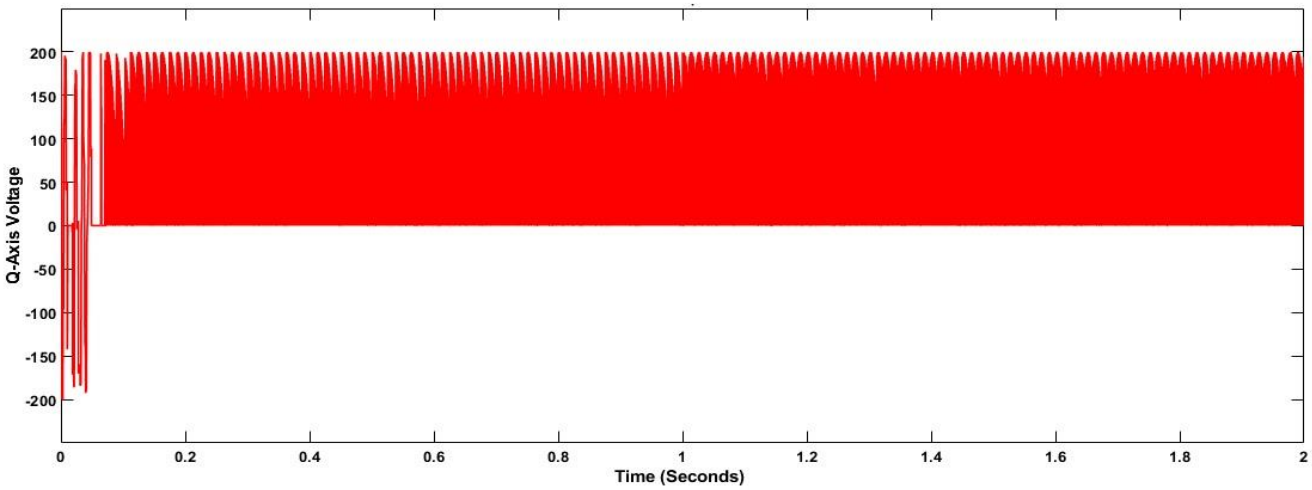

Figure 8.21 Simulation result of Q-axis voltage using modified duty ratio modulated -DTC

8.2.7 Observation

Speed- The steady state speed is achieved quickly in Duty Ratio Modulated -DTC compared to Modified Duty Ratio Modulated-DTC. But in the Modified Duty Ratio Modulated-DTC, the ripple is lesser than in Duty Ratio Modulated -DTC.

Torque- In Conventional DTC the torque ripple is quite high. But using Duty Ratio Modulation we can reduce the torque ripple to a decent level. But we can reduce the torque ripple more using the Modified Duty Ratio Modulation technique.

D-Q axis Current- Conventional Direct Torque Control Required more D-axis current than Duty Ratio Modulated -DTC and Modified Duty Ratio Modulated-DTC also the ripple is quite high. But Q axis current requirement is quite similar in all the control topologies. But ripple is lesser in Modified Duty Ratio Modulated-DTC compared to Duty Ratio Modulated -DTC and Conventional DTC.

D-Q axis voltage- Average value of D-axis voltage is more in the case of Conventional DTC. Q-axis voltage is rectified properly in the case of Modified Duty Ratio Modulated-DTC compared to the other two topologies.

8.3 Comparison of The Results and Discussion

Ripple Percentage (%)	Conventional-DTC	Duty Ratio Modulated -DTC	Modified Duty Ratio Modulated -DTC
Speed (Ref- 400 RPM)	0.4153	0.5355	0.2344
Torque (Ref-1 N-m)	24.54	14.68	7.17

Table 8.2 Ripple percentages of the response of different parameters

We can make the following decisions by looking at the ripple percentages listed in the previous table.

In the case of Conventional DTC, the speed ripple is 0.4153% but the ripple percentage gets a little bit higher (0.5355%) in the case of Duty ratio modulated DTC but for Modified method ripple percentage is quite low which is 0.2344%. It is the least among all. Despite the fact that our goal is to reduce torque ripple, the proposed scheme has achieved this goal as well because it has the best speed response of all the cases discussed here.

In the case of torque ripple, we can clearly observe that the torque ripple is quite low for the Modified method which is proposed here. It is about 7.17%. But for Duty ratio modulated DTC, it is 14.68% and for Conventional DTC, it is 24.54%. Therefore, our goal will be achieved if we employ Modified Duty Ratio Modulated-DTC because the torque ripple will be at its lowest.

Here, the responses to all three cases are presented and contrasted. The tables for each parameter include the ripple percentages. Here, the proposed scheme has the lowest speed and torque ripples. Overall, the Modified Duty Ratio Modulated-DTC method for controlling PMSM is much more effective than the other methods mentioned here.

Chapter 9

Conclusion

9.1 Contributions to the Work

Firstly, a literature survey related to the research area has been conducted and different vector control techniques for speed control of PMSM have been compared and studied.

In electric drives, PMSM is one of the most effective machines. So, it is used as this project's work plant. Also, PMSM has been studied with all the necessary equations and pertinent diagrams during this project.

PMSM is not self-starting. So, a three-Phase Voltage Source Inverter has been used to drive the PMSM. In order to do this, the theory of the Three-Phase Voltage Source Inverter with the necessary circuit diagram and tables has been studied.

After conducting studies on different types of speed control techniques it has been found that DTC is the most advantageous technique for speed control of PMSM. So, the theory of Direct Torque Control has been studied in detail with important equations, necessary tables, and relevant diagrams and the DTC technique is used for this project.

But, one major drawback for DTC is torque ripple. In order to reduce this ripple, various techniques are used. One of the most popular techniques is Duty ratio modulation. It is very easy to implement and it reduces the torque ripple significantly. So, the methodologies for duty ratio modulation have been studied and discussed with all formulas and necessary diagrams. Then, it has been used in the system to reduce the ripples.

For high-performance applications, the Duty ratio modulated DTC is again modified to obtain comparative less torque and flux ripple. In this thesis Duty ratio modulated DTC is associated with MTPA to reduce the torque ripple more. For this purpose, the MTPA technique was studied with all necessary formulas and implemented in this work.

The total system has been simulated in MATLAB software successfully and the response and ripple percentages have been compared. It has been found that the Modified Duty ratio Modulation Technique shows the best results among all the other cases.

9.2 Scopes of The Future Work

- Due to the simple structure of the proposed controller in this thesis, this can be implemented in hardware easily without using any expensive controller for further studies.
- Any other advanced controller can be attached along with this controller in order to reduce torque ripple more.
- The response obtained using other controllers can be compared with my work for further studies.
- This controller is robust enough so it can be used in practical work.

Appendix

Speed controller gain

K_p	6
K_i	2

Upper and lower limit of torque and flux hysteresis controller

$+T_H; -T_H$	0.2; -0.2
$+\Psi_H; -\Psi_H$	0.02; -0.02

Other parameters

Sample time (T_s)	12.5µs
Torque Limiter (T_{lim})	30
DC Voltage (V_{dc})	300V
C	0.001
Flux Reference (Ψ_{ref})	0.4
Reference speed (ω_{ref})	400 RPM
Starting load torque (T_L)	1 N-m
Load torque after 1 second (T_L)	5 N-m

References

[1] Krishnan R. “Electric Motor Drives Modelling, Analysis, and Control”. NJ, USA: Prentice Hall; 2011. p. 652.

[2] JACEK F. GIERAS, MITCHELL WING; “PERMANENT MAGNET MOTOR TECHNOLOGY Design and Application; *Second Edition*; Marcel Dekker, Inc.;2002; p.589.

[3] P. Pillay and R. Krishnan, "Modelling of permanent magnet motor drives," in *IEEE Transactions on Industrial Electronics*, vol. 35, no. 4, pp. 537-541, Nov. 1988, Doi: 10.1109/41.9176.

[4] D. Casadei, F. Profumo, G. Serra and A. Tani, "FOC and DTC: two viable schemes for induction motors torque control," in *IEEE Transactions on Power Electronics*, vol. 17, no. 5, pp. 779-787, Sept. 2002, Doi: 10.1109/TPEL.2002.802183.

[5] E. Ohno and M. Akamatsu, "Variable frequency SCR inverter with an auxiliary commutation circuit," in *IEEE Transactions on Magnetics*, vol. 2, no. 1, pp. 25-30, March 1966, Doi: 10.1109/TMAG.1966.1065792.

[6] B. Mokrytzki, "Pulse Width Modulated Inverters for AC Motor Drives," in *IEEE Transactions on Industry and General Applications*, vol. IGA-3, no. 6, pp. 493-503, Nov. 1967, Doi: 10.1109/TIGA.1967.4180823.

[7] I. Takahashi and T. Noguchi, "A New Quick-Response and High-Efficiency Control Strategy of an Induction Motor," in IEEE Transactions on Industry Applications, vol. IA-22, no. 5, pp. 820-827, Sept. 1986, Doi: 10.1109/TIA.1986.4504799.

[8] I. Takahashi and Y. Ohmori, "High-performance direct torque control of an induction motor," in IEEE Transactions on Industry Applications, vol. 25, no. 2, pp. 257-264, March-April 1989, Doi: 10.1109/28.25540.

[9] T. G. Habetler and D. M. Divan, "Control strategies for direct torque control using discrete pulse modulation," in IEEE Transactions on Industry Applications, vol. 27, no. 5, pp. 893-901, Sept.-Oct. 1991, Doi: 10.1109/28.90344.

[10] H. Y. Zhong, H. P. Messinger and M. H. Rashad, "A new microcomputer-based direct torque control system for three-phase induction motor," in IEEE Transactions on Industry Applications, vol. 27, no. 2, pp. 294-298, March-April 1991, Doi: 10.1109/28.73614.

[11] T. G. Habetler, F. Profumo, M. Pastorelli and L. M. Tolbert, "Direct torque control of induction machines using space vector modulation," in IEEE Transactions on Industry Applications, vol. 28, no. 5, pp. 1045-1053, Sept.-Oct. 1992, Doi: 10.1109/28.158828.

[12] M. P. Kazmierkowski and A. B. Kasprowicz, "Improved direct torque and flux vector control of PWM inverter-fed induction motor drives," in IEEE Transactions on Industrial Electronics, vol. 42, no. 4, pp. 344-350, Aug. 1995, Doi: 10.1109/41.402472.

[13] L. Zhong, M. F. Rahman, W. Y. Hu and K. W. Lim, "Analysis of direct torque control in permanent magnet synchronous motor drives," in IEEE Transactions on Power Electronics, vol. 12, no. 3, pp. 528-536, May 1997, Doi: 10.1109/63.575680.

[14] L. Zhong, M. F. Rahman, W. Y. Hu, K. W. Lim and M. A. Rahman, "A direct torque controller for permanent magnet synchronous motor drives," in *IEEE Transactions on Energy Conversion*, vol. 14, no. 3, pp. 637-642, Sept. 1999, doi: 10.1109/60.790928.

[15] Lixin Tang, Limin Zhong, M. F. Rahman and Yuwen Hu, "A novel direct torque control for interior permanent-magnet synchronous machine drive with low ripple in torque and flux-a speed-sensorless approach," in *IEEE Transactions on Industry Applications*, vol. 39, no. 6, pp. 1748-1756, Nov.-Dec. 2003, doi: 10.1109/TIA.2003.818981.

[16] D. Swierczynski and M. P. Kazmierkowski, "Direct torque control of permanent magnet synchronous motor (PMSM) using space vector modulation (DTC-SVM)-simulation and experimental results," IEEE 2002 28th Annual Conference of the Industrial Electronics Society. IECON 02, 2002, pp. 751-755 vol.1, doi: 10.1109/IECON.2002.1187601.

[17] S. Kouro, R. Bernal, H. Miranda, C. A. Silva and J. Rodriguez, "High-Performance Torque and Flux Control for Multilevel Inverter Fed Induction Motors," in *IEEE Transactions on Power Electronics*, vol. 22, no. 6, pp. 2116-2123, Nov. 2007, doi: 10.1109/TPEL.2007.909189.

[18] K. E. B. Quindere, F. E. Ruppert and F. M. E. De Oliveira, "A Three-Level Inverter Direct Torque Control of a Permanent Magnet Synchronous Motor," 2006 IEEE International Symposium on Industrial Electronics, 2006, pp. 2361-2366, doi: 10.1109/ISIE.2006.295941.

[19] Pengcheng Zhu, Yong Kang and Jian Chen, "Improve direct torque control performance of induction motor with duty ratio modulation," IEEE International Electric Machines and Drives Conference, 2003. IEMDC'03., 2003, pp. 994-998 vol.2, doi: 10.1109/IEMDC.2003.1210356.

[20] D. -H. Lee, Y. -J. An and E. -C. Nho, "A High-Performance Direct Torque Control Scheme of Permanent Magnet Synchronous Motor," *2007 7th International Conference on Power Electronics and Drive Systems*, 2007, pp. 1361-1366, doi: 10.1109/PEDS.2007.4487881.

[21] I. R. Akhil and C. K. Vijayakumari, "Modified Direct Torque Control scheme for PMSM," *2012 IEEE International Conference on Power Electronics, Drives and Energy Systems (PEDES)*, 2012, pp. 1-6, doi: 10.1109/PEDES.2012.6484328.

[22] A. Mohan, M. Khalid and A. C. Binojkumar, "Performance Analysis of Permanent Magnet Synchronous Motor under DTC and Space Vector-based DTC schemes with MTPA control," *2021 International Conference on Communication, Control and Information Sciences (ICCISc)*, 2021, pp. 1-8.

[23] H.F. Abdul Wahab and H. Sanusi "Simulink Model of Direct Torque Control of Induction Machine" American Journal of Applied Sciences 5 (8): 1083-1090, 2008 ISSN 1546-9239 © 2008 Science Publications.

[24] *Website*- https://www.linquip.com/blog/permanent-magnet-synchronous-motors

[25] *Website*- https://www.elprocus.com/what-is-a-permanent-magnet-synchronous-motor-itsworking/#:~:text=The%20working%20of%20PMSM%20depends,similar%20to%20brushless%20DC%20motors.

[26] Dmitry Levkin "Permanent magnet synchronous motor" engineering solutions. Available from: https://en.engineering-solutions.ru/motorcontrol/pmsm/#1

[27] Chafik Ed-dahmani, Hassane Mahmoudi and Marouane Elazzaoui “Direct Torque Control of Permanent Magnet Synchronous Motors in MATLAB/SIMULINK” 2nd International Conference on Electrical and Information Technologies ICEIT2016.

[28] P. Krause, O. Wasynczuk, Scott S., Steven P. “ANALYSIS OF ELECTRIC MACHINERY AND DRIVE SYSTEMS”, 3rd ed, “IEEE press series on Power engineering”, Wiley John & Sons; 2013.

[29] B.K. Bose,” Modern Power Electronics and AC Drives”, Pearson Education, 4th Edition, 2004.

[30] Turksoy, Omer & Yilmaz, Unal & Tan, Adnan & Teke, Ahmet. (2017). A Comparison Study of Sinusoidal PWM and Space Vector PWM Techniques for Voltage Source Inverter. Natural and Engineering Sciences. 2. 10.28978/nesciences.330584.

[31] Soe Sandar Aung, Thet Naing Htun "Speed Control System of Induction Motor by using Direct Torque Control Method used in Escalator"; International Journal of Trend in Scientific Research and Development (ijtsrd), ISSN: 2456-6470, Volume-3; Issue-5, August 2019, pp.2250-2253.

[32]. Mukesh Kumar Arya, DR. Sulochona Wadhwani, “DEVELOPMENT OF DIRECT TORQUE CONTROL MODEL WITH USING SVI FOR THREE PHASE INDUCTION MOTOR”, International Journal of Engineering Science and Technology (IJEST); Vol. 3, Issue-8; August 2011.

[33] M. N. A. Kadir, S. Mekhilef and W. P. Hew, "Comparison of Basic Direct Torque Control Designs for Permanent Magnet Synchronous Motor," 2007 7th International Conference on Power Electronics and Drive Systems, 2007, pp. 1344-1349.

[34] Zhuqiang Lu, Honggang Sheng, H. L. Hess and K. M. Buck, "The modelling and simulation of a permanent magnet synchronous motor with direct torque control based on Matlab/Simulink," *IEEE International Conference on Electric Machines and Drives, 2005.*, 2005, pp. 7 pp.-1156.

[35] M. A. M. Cheema, J. E. Fletcher, D. Xiao and M. F. Rahman, "A Direct Thrust Control Scheme for Linear Permanent Magnet Synchronous Motor Based on Online Duty Ratio Control," in *IEEE Transactions on Power Electronics*, vol. 31, no. 6, pp. 4416-4428, June 2016.

[36] Mosaddegh Hesar, H., Abootorabi Zarchi, H. and Ayaz Khoshhava, M. (2019), Online maximum torque per ampere control for induction motor drives considering iron loss using input-output feedback linearization. IET Electric Power Applications, 13: 2113-2120.

[37] https://in.mathworks.com/help/mcb/gs/field-weakening-control-mtpa-pmsm.html

[38] https://in.mathworks.com/help/mcb/ref/mtpacontrolreference.html